Cancer Letters 520 (2021) 184–200

Contents lists available at ScienceDirect

Cancer Letters

journal homepage: www.elsevier.com/locate/canlet

Stromal fibroblasts shape the myeloid phenotype in normal colon and colorectal cancer and induce CD163 and CCL2 expression in macrophages

Mira Stadler [a,1,2], Karoline Pudelko [a,1,3], Alexander Biermeier [a,1], Natalie Walterskirchen [b,1], Anthoula Gaigneaux [c], Claudia Weindorfer [a], Nathalie Harrer [d], Hagen Klett [e], Markus Hengstschläger [a], Julia Schüler [e], Wolfgang Sommergruber [d,1], Rudolf Oehler [b], Michael Bergmann [b], Elisabeth Letellier [c], Helmut Dolznig [a,*]

[a] Institute of Medical Genetics, Medical University of Vienna, Währinger Straße 10, A-1090 Vienna, Austria
[b] Department of Surgery, Medical University of Vienna, Währinger Gürtel 20, A-1090 Vienna, Austria
[c] Department of Life Sciences and Medicine, University of Luxembourg, 6 Avenue du Swing, L-4367, Campus Belval, Luxembourg
[d] Boehringer Ingelheim RCV GmbH & Co KG, Vienna, Austria, Dr. Boehringer-Gasse 5-11, A-1130 Vienna, Austria
[e] Charles River Research Services Germany GmbH, Am Flughafen 12-14, 79108 Freiburg, Germany

ARTICLE INFO

Keywords:
Cancer associated fibroblasts
Colon cancer
CCL2
Immune cell recruitment and polarization
Tumor microenvironment

ABSTRACT

Colorectal cancer (CRC) accounts for about 10% of cancer deaths worldwide. Colon carcinogenesis is critically influenced by the tumor microenvironment. Cancer associated fibroblasts (CAFs) and tumor associated macrophages (TAMs) represent the major components of the tumor microenvironment. TAMs promote tumor progression, angiogenesis and tissue remodeling. However, the impact of the molecular crosstalk of tumor cells (TCs) with CAFs and macrophages on monocyte recruitment and their phenotypic conversion is not known in detail so far.

In a 3D human organotypic CRC model, we show that CAFs and normal colonic fibroblasts are critically involved in monocyte recruitment and for the establishment of a macrophage phenotype, characterized by high CD163 expression. This is in line with the steady recruitment and differentiation of monocytes to immunosuppressive macrophages in the normal colon. Cytokine profiling revealed that CAFs produce M-CSF, and IL6, IL8, HGF and CCL2 secretion was specifically induced by CAFs in co-cultures with macrophages. Moreover, macrophage/CAF/TCs co-cultures increased TC invasion. We demonstrate that CAFs and macrophages are the major producers of CCL2 and, upon co-culture, increase their CCL2 production twofold and 40-fold, respectively. CAFs and macrophages expressing high CCL2 were also found *in vivo* in CRC, strongly supporting our findings. CCL2, CCR2, CSF1R and CD163 expression in macrophages was dependent on active MCSFR signaling as shown by M-CSFR inhibition.

These results indicate that colon fibroblasts and not TCs are the major cellular component, recruiting and dictating the fate of infiltrated monocytes towards a specific macrophage population, characterized by high CD163 expression and CCL2 production.

1. Introduction

Macrophages are mononuclear phagocytes and part of the innate immune system [1]. Their main function is phagocytosis, antigen presentation, cytokine secretion, generation and resolution of inflammation. They play a critical role in tissue homeostasis, immunity and are involved in a wide range of pathologies such as cancer and fibrosis [2]. The gastrointestinal immune compartment holds a special position in

* Corresponding author.
E-mail address: helmut.dolznig@meduniwien.ac.at (H. Dolznig).
[1] equally contributing first authors, listed in order of their timely involvement in the project.
[2] Institute of Pathology, Medical University of Vienna, Währinger Gürtel 20, A-1090 Vienna, Austria.
[3] Universitätsmedizin Göttingen, Georg-August-Universität, Robert-Koch-Straße 40, 37075 Göttingen, Germany.
[4] Department of Biotechnology, University of Applied Sciences, Helmut-Qualtinger-Gasse 2, A-1030 Vienna, Austria.

https://doi.org/10.1016/j.canlet.2021.07.006
Received 19 April 2021; Received in revised form 1 July 2021; Accepted 2 July 2021
Available online 10 July 2021

the body since it is exposed to an extraordinary bacterial load. It has to discriminate between harmless antigens from commensal bacteria keeping the inflammatory response low but effectively fighting potentially dangerous pathogens. Therefore, immune cell regulation in these tissues is believed to differ fundamentally from other organs. In the healthy intestine, tissue-resident macrophages arise continuously from $CD14^+$ blood monocytes [3,4]. Regarding the short half-life of about two-three weeks [5], constant monocyte recruitment, predominantly via the CCL2/CCR2 axis, is essential to maintain homeostasis of intestinal macrophages. Tissue resident macrophages from healthy lamina propria are $CD68^+$/$CD163^+$/$CD163L1^+$/$CD206^+$ [1] and exhibit luminal antigen sampling, bacterial and apoptotic cell clearing as well as antigen presenting and antigen transfer function. Moreover, they support epithelial barrier function and help to expand regulatory T cells and Th17 cells [6]. We avoid the terms M1 and M2 macrophages, as recent single cell sequencing approaches of various cancers and the corresponding normal tissues revealed that macrophage subtypes present in tumors neither match the criteria of dichotomous M1/M2 phenotypes nor the proposed continuum of intermediates between the two states [7–9].

Macrophages also represent the main immune cell component in colorectal cancer (CRC), which is the 3rd most common cancer in the western world accounting for about 10% of cancer deaths [10]. It is well accepted that colon carcinogenesis is influenced by the tumor microenvironment, mainly by cancer associated fibroblasts (CAFs). They secrete high levels of cytokines, chemokines and growth factors, thereby they can promote angiogenesis, tumor growth and influence pro-and anti-tumor immune response. A high CAF signature present in CRC is highly predictive for poor prognosis [11,12].

CRCs are also heavily infiltrated by macrophages, which predominantly reside in the tumor stroma and not in the tumor epithelial compartment [13], suggesting that signals from CAFs might recruit and retain them in the tumor microenvironment. However, many cellular and molecular mechanisms of macrophage recruitment and function are still unclear, particularly for the impact of macrophages in CRC. In contrast to many other cancers (breast, gastric, ovarian etc), high total macrophage infiltration (defined by $CD68^+$ cells) is correlated with favorable prognosis [14–16], whereas elevated $CD163^+$ TAM numbers were inconsistent predictors and correlated with poor [17,18] or advantageous prognosis [19].

However, there is ample evidence from experimental mouse models demonstrating the critical involvement of macrophages in colon cancer initiation [20,21] and progression [22]. Macrophages support angiogenesis, tumor cell migration and invasion and provide an immunosuppressive microenvironment to suppress anti-tumor immune response. (PMID: 20371344). Most evidently, interruption of monocyte recruitment by CCL2/CCR2 axis intervention or macrophage differentiation and survival by MCSF/CSF1R inhibition [23] has a tumor reducing effect. For example, CCL2 inhibition by CCR2 knockout reduces colitis-associated carcinogenesis in mice [24]. In line with these observations, CSF-1 (M-CSF) and CCL-2 overexpression is associated with poor prognosis in colorectal cancer [25,26].

Thus, it is essential to better understand the biology of human macrophages in the normal gut and in the TME and their contribution to cancer progression. The crosstalk of fibroblasts with macrophages has not been addressed in detail so far in CRC. We show here that CAFs play an essential role in the recruitment and polarization of both macrophages and circulating monocytes and the interaction of CAFs with macrophages drastically induces colon cancer cell invasion. Moreover, we show that CCL2 and M-CSF are predominantly derived from CAFs.

2. Materials and methods

2.1. Cells

Human colon cancer cell lines HCT116 (CCL-247™) and DLD-1 (CCL 221™) obtained from the American Type Culture Collection (ATCC® Rockville, MD, US) were cultured in Dulbecco's modified Eagle Medium (DMEM) with 10% fetal calf serum (FCS, HI, Gibco, Thermo Fisher Scientific, Waltham, MA, US), 1% L-glutamine (Gln), 1% penicillin/streptomycin (PenStrep). Primary cancer associated fibroblasts (CAFs) and normal colon fibroblasts (NAFs) were previously isolated from colon carcinomas and matched normal colon tissue from the same patients [27]. In this study CAF3/NAF3, CAF28/NAF28 and CAF34/NAF34 pairs and CAF4 from different patients were used. Fibroblasts were cultured in endothelial growth medium (EGM-2MV, PromoCell, Heidelberg, Germany) and used at low passage numbers (p3-p12) as described [28]. Peripheral blood mononuclear cells (PBMCs) were isolated from human peripheral blood of healthy donors.

2.2. Isolation and differentiation/polarization of human blood monocytes

PBMCs were isolated according to established protocols using Ficoll Paque Premium (GE Healthcare) density gradient centrifugation. Monocytes were isolated from PBMCs by adherence to non-treated culture dishes and used directly or differentiated into macrophages (M_{MCSF}) for 6 days in RPMI/10% FCS, 1% Gln, 1% PenStrep and 20 ng/ml human recombinant M-CSF (Peprotech, Rocky Hill, NJ, US) with one medium change. Macrophages were either used unpolarized (M_{MCSF}) or were polarized in DMEM + 2% FCS, 1% Gln, PenStrep and 100 ng/ml LPS and 20 ng/ml IFNγ ($M_{LPS/IFN\gamma}$). Alternative activation was achieved in DMEM/2% FCS/1% Gln/1% PenStrep and 20 ng/ml IL-4 (Peprotech) for 48h ($M_{IL\text{-}4}$).

2.3. Collagen gel cultures

Collagen gel cultures were setup as described [27]. In brief, 2×10^3 colon cancer cells, 2×10^5 fibroblasts and 2×10^5 monocytes or macrophages were introduced into collagen I gels (rat tail collagen I, Corning Inc, #354236; final conc. 2 mg/ml) in mono-, double-and triple-cultures. Conditioned media (CM) were collected. The cells were cultured for 5–7 days with partial medium change (50%) every other day. Gels were used for flow cytometry, mRNA isolation, or were formalin fixed and paraffin embedded (FFPE), cut and Hematoxylin and Eosin (H&E) and immunohistochemically (IHC) stained. Raft culture assays were performed as described [28] with addition of monocytes or macrophages (2×10^6) into the collagen gels. Gels were incubated for 10 days at the air liquid interface, fixed and cut perpendicular.

2.4. Monocyte and macrophage attraction Assay/Tumor cell migration

The CM from 3D collagen gel cultures were used for monocyte and macrophage recruitment assays. Transwell inserts (5 μm pore size) were placed into 24-well plates and 5×10^4 monocytes or macrophages were seeded in 100 μl serum free DMEM into the upper chamber. Cells migrated towards the varying CM mixed 1:1 with DMEM/2% FCS. DMEM/1% FCS was used as control. After 24h, the migrated cells on the undersurface of the membranes and in the wells were stained with calcein for 1h at 37°, harvested by detachment/scraping and transferred into 96-well plates, centrifuged and the fluorescence was measured in a Biotek Synergy reader. Tumor cell migration assays were performed as described above, except for using 8 μm pore size and cells at the membrane undersurface were taken into account. Quantification of the migrated cells was done by DAPI staining, using microscopic imaging.

2.5. Tumor cell invasion

Spheroids (3×10^3 cells/spheroid) were formed from HCT116 cells, which ectopically express EGFP (HCT116-GFP) by seeding into non-adhesive U-shaped 96-well plates in DMEM/5% FCS. After 3 days spheroids were harvested and introduced (48 spheroids/gel) into collagen gels in mono-, double- and triple-cultures together with

fibroblasts and macrophages. The medium was changed every 2–3 days and pictures were taken after every 24 h. Invasion was determined by counting GFP^+ structures extending form the spheroids into the collagen gels.

2.6. Immunofluorescence on FFPE tissues

Sections (4 μm) of formalin fixed, paraffin embedded (FFPE) human CRCs were deparaffinized, rehydrated and citrate antigen retrieval was performed. Samples were blocked and stained o/n with primary antibody (CCL2, CD68) and subsequently with fluorescently labeled secondary antibody (1:500) for 45 min. Corresponding IgG antibodies were used as controls. Confocal Laser Scanning Microscope analysis (Leica TCS SP8; Leica Application Suite X, Leica, Wetzlar, Germany) was performed using maximum projection of z-stacks (10 optical sections in 3 μm stack size) and analyzed in FIJI. 15 regions of interest (ROIs) were defined/field representing one single cell, which was identified by nuclear DAPI stain. Macrophages were identified by CD68, CCL2 expression was monitored in either $CD68^+$cells or $CD68^-$ elongated cells in the stroma. RGB mean fluorescence intensities (MFI) were calculated for every ROI and MFI of IgG controls (10 ROIs) were subtracted.

2.7. Immunofluorescence of collagen gels

For collagen gels, prior to the staining, the cells were treated with 10 μg/ml Brefeldin A for 4 h, fixed in Roti® Histofix 4% for 10 min at RT. Gels were washed 3x in TBS-T (0.5% Tween®20) and 3x in PBS-T and blocked in PBS-T/1% BSA for 1 h at RT. Thereafter, the gel was stained in 100 μl blocking solution with pre-labeled Alexa Fluor® 488 anti-CD68 (1:100), PE anti-CCL2 (1:50) and Alexa Fluor® 647 anti-Vimentin (1:1000) overnight at 4 °C. After washing in PBS-T, 100 μl of DAPI solution (2 μg/ml) was added for 45 min at RT and washed. The gel pieces were transferred to microscope slides in Vectashield® mounting medium, cover-slipped and analyzed on a Leica SP8 DM6000 CFS confocal microscope.

2.8. Flow cytometry

For CCL2 flow cytometry, prior to flow cytometry analysis, the cells were treated with 10 μg/ml Brefeldin A for 4 h. All other analyses were carried out without Brefeldin pretreatment. Cells in 2D were washed and scraped for harvesting, whereas collagen gel co-cultures were collagenase B digested (1:8) in 1x DPBS (with Ca and Mg) for 10 min at RT. Collagenase was inhibited by 1:1000 0.5 M EDTA pH8 and cells were washed and resuspended in DPBS/2% FCS. Human TruStain FcX™ (1:20) was added for 15 min at RT to block Fc receptors. After staining with Alexa Fluor® 647 conjugated antibody against CD163 (1:100) the cells were fixed and permeabilized with Fix&Perm® and stained with anti-CD68-Alexa Fluor® 488 (1:100) or anti-CD45-BV421 (1:50), anti-CCL2-PE (1:50) and anti-Vimentin-Alexa Fluor® 405 (1:300) or APC-*anti*-CCR2 (1:100), anti-MCSFR-PE (1:50). Vimentin and CD68 were used to identify and gate the three distinct cell populations in the cultures: macrophages: Vim+/CD68+, fibroblasts: Vim+/CD68-, tumor cells: Vim-/CD68-). Protein expression was quantified using the mean fluorescence intensity (MFI). All flow cytometry data were obtained with CytoFLEX S (Beckman Coulter, AS38034) and analyzed with FlowJo_V10. CCL2, CCR2, CD45, CD68, CD163 antibodies were from Biolegend (San Diego, CA, US); CCR2 and MCSFR antibodies were from R&D Systems; vimentin antibodies were purchased from abcam (Cambridge, UK).

2.9. Cytokine profiling

The "Human Cytokine XL array (R&D Systems) and the "Cytokine Human Magnetic 30-Plex Panel" for Luminex™ Platform (Thermo Fisher Scientific, #LHC6003 M) was used to quantify cytokines, chemokines and growth factors in the CM from the 3D collagen gel cultures. For both methods, all buffers, solutions and samples were prepared and the assays were performed according to protocol. The sample concentrations in the Luminex setup were determined from standard curves using curve fitting software.

2.10. CCL2 enzyme linked immunosorbent assay (ELISA)

CCL2 ELISA was conducted according to ELISA MAX™ Deluxe Set Human MCP-1/CCL2 protocol (R&D Systems Inc, Minneapolis, MN, US). Briefly, uncoated 96-well plates were incubated 16–18 h prior to running the ELISA with capture antibody at 4 °C. After washing, the plate was blocked, washed again and 100 μl of standard/sample was added to the wells and incubated for 2 h shaking at RT. After a further washing step, the detection antibody for CCL2 was added and incubated for 1 h shaking at RT. Avidin-HRP solution was added for 30 min and after a final wash step 100 μl of TMB substrate solution was added in the dark for 20 min, stopped and measured with a BioTek Synergy ™ HT Multi-Detection Microplate Reader (BioTek Instruments, Winooski, VT, US) using the Gen5 Microplate Reader and Imager Software. Absorbance at 570 nm was subtracted from 450 nm.

2.11. Expression profiling data

Data were derived from expression-profiling screens of dissected human CRC specimens performed earlier from Rupp [29], Nishida, GSE3560216 [30]; Calon, GSE3939718 [12]; Isella, GSE56699 [11] using the Geo2R web application or of cell culture datasets from Dolznig [27] and Qiao [31] and visualized in GraphPad Prizm.

2.12. RNA seq of human CRC patient derived xenograft (PDX) models

Total RNA from PDX tumors was isolated, DnaseI (NEB) digested and purified by oligo-dT beads (Dynabeads mRNA purification kit, Invitrogen). Then poly(A)-containing mRNA were fragmented into 200-250bp with Fragment buffer (Ambion). Sequencing libraries were prepared and validated following the sequencing provider's RNA-Seq protocols. Sequencing was done using Illumina HiSeq-2000/2500/4000 and Novaseq 6000 in 100/126/150 bp paired-end (PE) reads with an expected throughput of 10G – 18G bases per sample.

To distinguish between human and mouse reads, *xenome* [32] was utilized classifying reads into human, mouse, both or ambiguous. Using only human (mouse) reads, we performed alignment against the reference GRCh38 (GRCm38) with *hisat2* [33]. Subsequently normalized gene expression (TPM) was obtained by matching mapped reads to Gencode v27 (Gencode vM20) using *stringtie* [34]. This dataset is called Charles River Research Services Germany (CRRSG) dataset here.

2.13. Single cell mRNA sequencing dataset analysis

Single cell data from the Smart-seq2 dataset [8] were used. The dataset contains 10468 cells, annotated with cluster and tissue metadata. TPM values and metadata were retrieved from GEO (GSE146771) and analyzed using R [35] and bioconductor [36] environment. TPM were processed (log transformed and size factor adjusted) and graphed using monocle3 library [37–39].

3. Results

3.1. Modular three-dimensional organotypic models of colon cancer to mimic tumor cell, cancer associated fibroblast and macrophage interaction

In order to recapitulate human colon cancer biology with a special focus on the tumor microenvironment (TME), we used three-dimensional (3D) organotypic assays (OTAs) [27]. We were specifically interested in the interaction of tumor cells, fibroblasts and

monocytes/macrophages. In a modular setup colon tumor cells (T, HCT116) were cultivated in 3D collagen gels either alone or in co-culture with cancer associated fibroblasts (CAF, C) and/or macrophages (M) or monocytes (Fig. 1A). This modularity has one advantage compared to *in vivo* experiments, which is the possibility to analyze different components of a cancer individually or in each possible combination. Thus, this experimental setup allowed the evaluation of phenotypic and molecular changes, which occurred in double and triple organotypic co-cultures in comparison to individual monocultures. For this, the OTAs were cultivated for 5–10 days with regular partial medium changes (every 48 h). We evaluated cancer cell invasion and used conditioned media (CM) from the 3D cultures to investigate the impact of the individual cell types and their combinations on monocyte recruitment and cytokine composition. Moreover, macrophages isolated from these gels were investigated for their phenotype.

Phase contrast microscopy revealed that HCT116 tumor cells (T) alone formed spheroid structures in the gels after 7 days, whereas macrophages (M) displayed elongated and stellate structures and CAFs (C) displayed a predominantly spindle-like and occasional stellate phenotype. HCT116 cells in combination with macrophages (T + M) and or CAFs (T + C) displayed invasive, astral outgrowth (Fig. 1B).

Next, we analyzed the phenotypic appearance of the myeloid cells -derived from peripheral blood monocytes - cultivated in monoculture and different co-culture raft culture assays (Suppl. Fig. S1). Intriguingly, the morphology of the myeloid cells closely resembled macrophages in human colon cancer stroma, displaying an either elongated or stellate-like cell phenotype (Fig. 1C). These macrophages were predominantly present in the stromal compartment of the cultures and rarely invaded into the tumor cell layer (Suppl. Fig. S2).

3.2. *The presence of CAFs induce monocyte differentiation and the establishment of a CD68^{+}/CD163^{high} macrophage phenotype*

The monocyte-derived cells were positive for CD68 and CD163 (Suppl. Fig. S2A). When using MCSF pre-differentiated macrophages in 2D (designated here M_{MCSF}) as input for the OTA cultures, the same

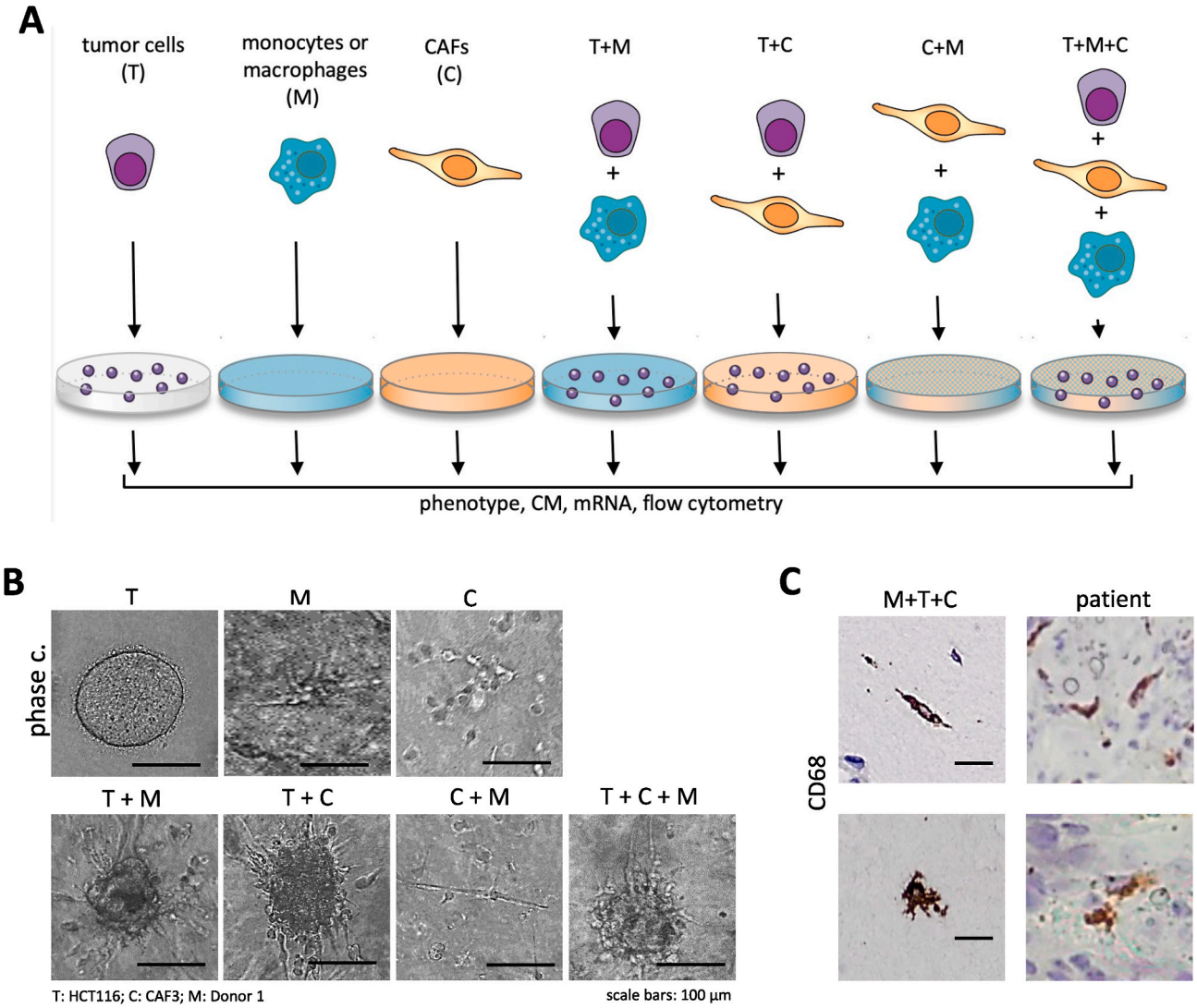

Fig. 1. ***Organotypic models of colon cancer to investigate tumor cell, cancer associated fibroblast (CAF) and macrophage interaction.*** **A** Model. 2×10^3 colon cancer cells (T, HCT116), 2×10^5 fibroblasts (F, NAFs/CAFs) and 2×10^5 monocytes (Mo) isolated from human peripheral blood or monocyte-derived macrophages (M) were introduced into collagen I gels in mono-, double-and triple-cultures in triplicates. After 5 days conditioned media (CM) were collected and individual gels of the same conditions were used for flow cytometry, mRNA isolation, or were formalin fixed and paraffin embedded (FFPE), cut and Hematoxylin and Eosin (H&E) and immunohistochemically (IHC) stained. **B** Representative phase contrast images of HCT116 (T), CAFs (CAF3, C) and macrophages (M) after 5 days in mono- and co-cultures. **C** Macrophages (M, input 2×10^5 monocytes) identified by the pan macrophage marker CD68 (brown IHC staining) in sections of triple raft culture with 1.25×10^6 tumor cells and 2×10^5 CAFs, in comparison to CD68^{+} cells in sections of a primary patient CRC. Elongated and stellate-like phenotypes are recognizable.

phenotype was evident (Suppl. Fig. S2B). Thus, we concluded that monocytes differentiated to macrophages in the course of collagen gel culture within five to seven days.

Interestingly, conditioned media from CAF-containing OTA cultures was sufficient to induce an increase of CD163 expression in peripheral monocyte cultures in 2D after two days (Suppl. Fig. S3). These results were recapitulated in mono-, co- and triple culture OTAs. After five days of culture the collagen gels were digested and single cell suspensions were recovered. They were quantitatively evaluated by flow cytometry (Fig. 2A and B; gating: Suppl. Fig. S4). As expected, tumor cells (T) and CAFs (C) were negative for CD68 and CD163 expression in monocultures as well as in co-cultures. Monocytes developed into $CD68^{+}$ cells and displayed variable CD163 expression dependent on the culture conditions. In gels containing CAFs (M + C, M + T + C), the mean fluorescence intensities (MFI) of CD163 on the myeloid cells increased about threefold (Fig. 2B) as compared to mono-culture (M) or tumor cell co-culture (M + T). Another evaluation, dividing the myeloid cells into CD163-low, -medium and -high expressors revealed similar results (Fig. 2C). The same results were obtained when predifferentiated M_{MCSF} macrophages were used as input (Fig. 2D, Suppl. Fig. S5).

In order to demonstrate that fibroblast-dependent upregulation of CD163 expression in the macrophages was a general event, three different monocyte donors, two tumor cell lines and two CAF cultures from different patients were used. All showed consistent induction of CD163 in the presence of fibroblasts (Fig. 2E, Suppl. Fig. S6). Even the input of LPS/IFNγ pre-polarized macrophages resulted in elevated CD163 levels after co-culture with the CAFs (Fig. 2E, right panels, Suppl. Fig. S7).

Hence, we concluded that CAFs and to a certain extend also NFs shape a specific macrophage polarization state which is characterized by high CD163 expression, whereas tumor cells have no impact on this phenotype.

3.3. CAF/macrophage co-cultures lead to elevated colon cancer cell invasion

Next, cancer cell invasion was evaluated in our *in vitro* assays in more detail. After 7 days of culture, H&E (Fig. 3A) and cytokeratin 18 (CK18, Fig. 3B) stained sections of the gels revealed tumor cell invasion, when HCT116 (T) tumor cells were co-cultivated with M or C, and invasion reached a maximum in M + C + T co-cultures. HCT116 cell clusters in monoculture displayed no signs of invasion. Raft culture assays revealed similar results (Suppl. Fig. S8A). In order to quantify tumor cell invasion, we made use of HCT116-GFP cells, which were induced to form spheroids and were embedded into collagen gels in the presence or absence of C, M or C + M in the gels. After 24 h GFP positive invasive structures (Fig. 3C) per spheroid were identified and quantified (Fig. 3D). In line with the previous experiments, HCT116 spheroids in monoculture did not show any signs of migratory cells. Macrophages induced low levels of invasion in HCT116 spheroids, whereas CAFs had a significantly more pronounced effect. The triple culture was most effectively inducing cancer cell invasion. In line with published results, patient matched normal colon fibroblasts (NFs, N) induced less tumor cell invasion than CAFs, which was not further elevated by the addition of macrophages (Fig. 3D).

These results were confirmed by transwell migration of HCT116 cells towards CM of the different mono-, co- and triple cultures (Suppl. Fig. S8B). Thus, we demonstrate the induction of a pro-migratory and pro-invasive phenotype of tumor cells by CAFs and macrophages with different models and experimental readouts.

3.4. CAF-derived factors are major contributors to monocyte attraction

Next, we addressed whether monocyte migration towards factors released by the various cell types, or the co- or triple-cultures was different. In transwell migration assays, monocytes were seeded into the upper chamber of transwell inserts and were allowed to migrate for 24 h towards the varying conditioned media (CM). Surprisingly, CAF-CM was most competent in attracting monocytes, displaying an about fourfold increase as compared to macrophage or tumor cell CM (Fig. 4A). Similarly, CM from CAFs in double- and triple-cultures with macrophages and tumor cells, display significantly enhanced migration efficiency, in contrast to CM from co-cultures without CAFs. Under homeostatic conditions there is continuous monocyte recruitment into the normal intestine [4]. Based on the results from CAFs we hypothesized that normal colon fibroblasts might be responsible for the steady recruitment into the healthy colon. Thus, we investigated whether monocyte motility was differentially induced by CM from NF or CAF monocultures. For this, patient-matched NF/CAF pairs were analyzed. Indeed, the CM from NF and CAF cultures were equally potent to attract monocytes (Fig. 4B). Similar results albeit at lower amplitude were obtained if MCSF-derived macrophage (M_{MCSF}) migration was analyzed (Suppl. Fig. S9).

These results demonstrate that fibroblasts are the cells responsible for monocyte/macrophage recruitment/retention *in vitro*. Thus, we concluded that CAF-derived factors are critically involved in recruitment and regulation of monocyte/macrophage functions.

3.5. Cytokine profiling of macrophage, CAF and cancer cell mono-, co- and triple-cultures

Monocyte recruitment and macrophage polarization is critically dependent on released cytokines and growth factors. Thus, we aimed to get a deeper insight into the secreted molecules induced by certain cell-cell interactions in the OTAs. Therefore, we analyzed the levels of common cytokines and growth factors in the supernatants of *3D in vitro* mono-, double- and triple-cultures by cytokine arrays (Fig. 4C and D; Suppl. Tables S1 and S2) and multiplex bead ELISAs (Fig. 4E and F). We identified interesting regulated cytokines and growth factors such as M-CSF (CSF1), CCL2, HGF, IL6 and IL8 (Fig. 4F). High levels of M-CSF (3 ng/ml/48 h) were predominantly secreted by CAFs in monoculture, whereas tumor cells secreted 10 times less M-CSF and macrophages alone were almost negative for its secretion. In CAF containing double and triple cultures M-CSF levels were similar to the CAF monocultures and if CAFs were not present the levels remained low. Thus, this pattern suggests that CAFs are the main source of M-CSF in our physiologic *in vitro* cancer model irrespective of the interaction with other cell types.

IL6 was selectively secreted by CAFs in monocultures. This is consistent with many reports in the literature placing CAFs as major producers of IL6 in the tumor microenvironment of many cancers [40, 41]. Interestingly, macrophage and tumor cell co-cultures, despite being negative as monocultures, showed elevated levels of IL6 production. This was also evident when CAFs were co-cultivated with macrophages leading to an increase of IL6 secretion compared to CAF cultured alone. Surprisingly, the triple cultures displayed a synergistic increase in IL6 levels (2.5 ng/ml) reaching about twice the level of adding up the double-cultures. Therefore, in this situation the cross talk of the three cell types is essential to reach high levels of IL6 secretion. The same was true for IL8 production; again, the triple culture displayed high levels (20 ng/ml), whereas monocultures and co-cultures showed lower IL8 levels.

CCL2 showed a very interesting mode of expression. In monocultures, CCL2 levels were low to absent in macrophages and tumor cells, whereas CAFs showed considerable CCL2 secretion (375 pg/ml). In contrast, when macrophages were co-cultured with tumor cells or CAFs, CCL2 levels increased drastically into the range of nanogram levels per milliliter. In triple cultures, the quantities were further increased and reached 4.5 ng/ml. Since CCL2 is a major factor for monocyte recruitment and myeloid cell function [42] and displayed this interesting pattern of secretion we further focused on CCL2. Conventional ELISA confirmed the pattern of expression in a number of biological replicates and further substantiated the observation that

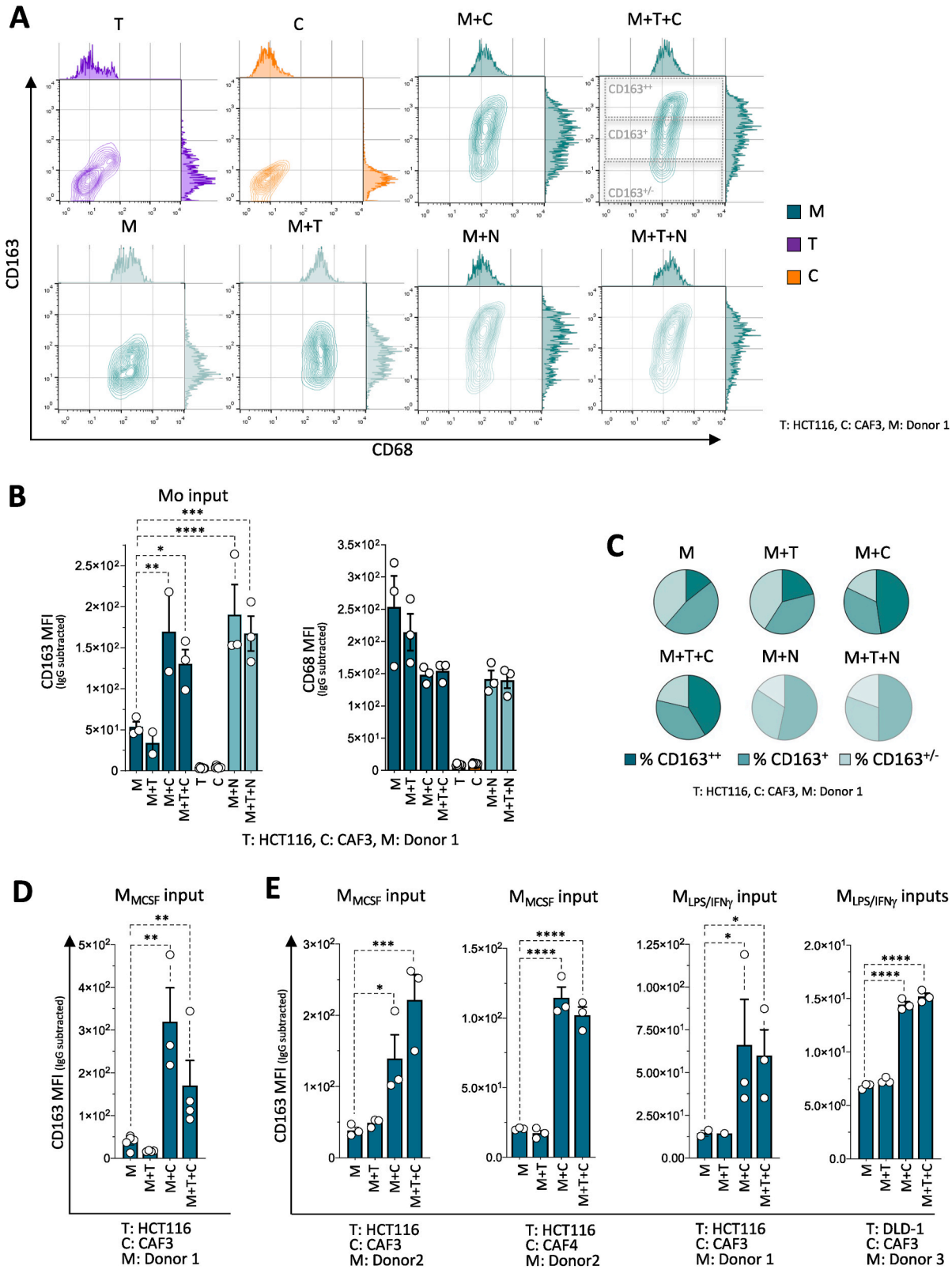

Fig. 2. ***Determination of macrophage phenotype from collagen gel cultures by flow cytometry.*** **A** Monocytes (Mo) isolated from human peripheral blood and primary CAFs (C) as well as tumor cells (T, HCT116) were introduced into collagen gels in mono-, double- and triple-cultures. Cancer cells, fibroblasts and macrophages (M) were isolated from collagen gels after 5 days in mono- and co-cultures. For FACs analysis cells were stained against the pan-macrophage marker CD68 (for gating) and CD163. T (tumor cells, HCT116); C (fibroblasts, CAF3); N (normal fibroblasts, NF3); M (macrophages) **A** Representative CD68/CD163 scatter plots **B** CD163 and CD68 mean fluorescence intensities (MFI) are illustrated. Corresponding IgG staining was subtracted from the MFI; **C** The mean percentages of $CD163^{low/medium/high}$ macrophages (from B) are indicated in pie charts. **D**, **E** CD163 MFIs in macrophages are indicated in bar graphs. Different monocyte donors and pre-polarized macrophages (M_{MCSF}, $M_{LPS/IFN\gamma}$), CAFs and tumor cells were used as indicated. For B, D, E: individual values as white dots; min n = 3; error bars represent SEM, p-values from one way ANOVA (Tukey's multiple comparisons) are shown. P values: *<0.05, **<0.01, ***<0.001, ****<0.0001.

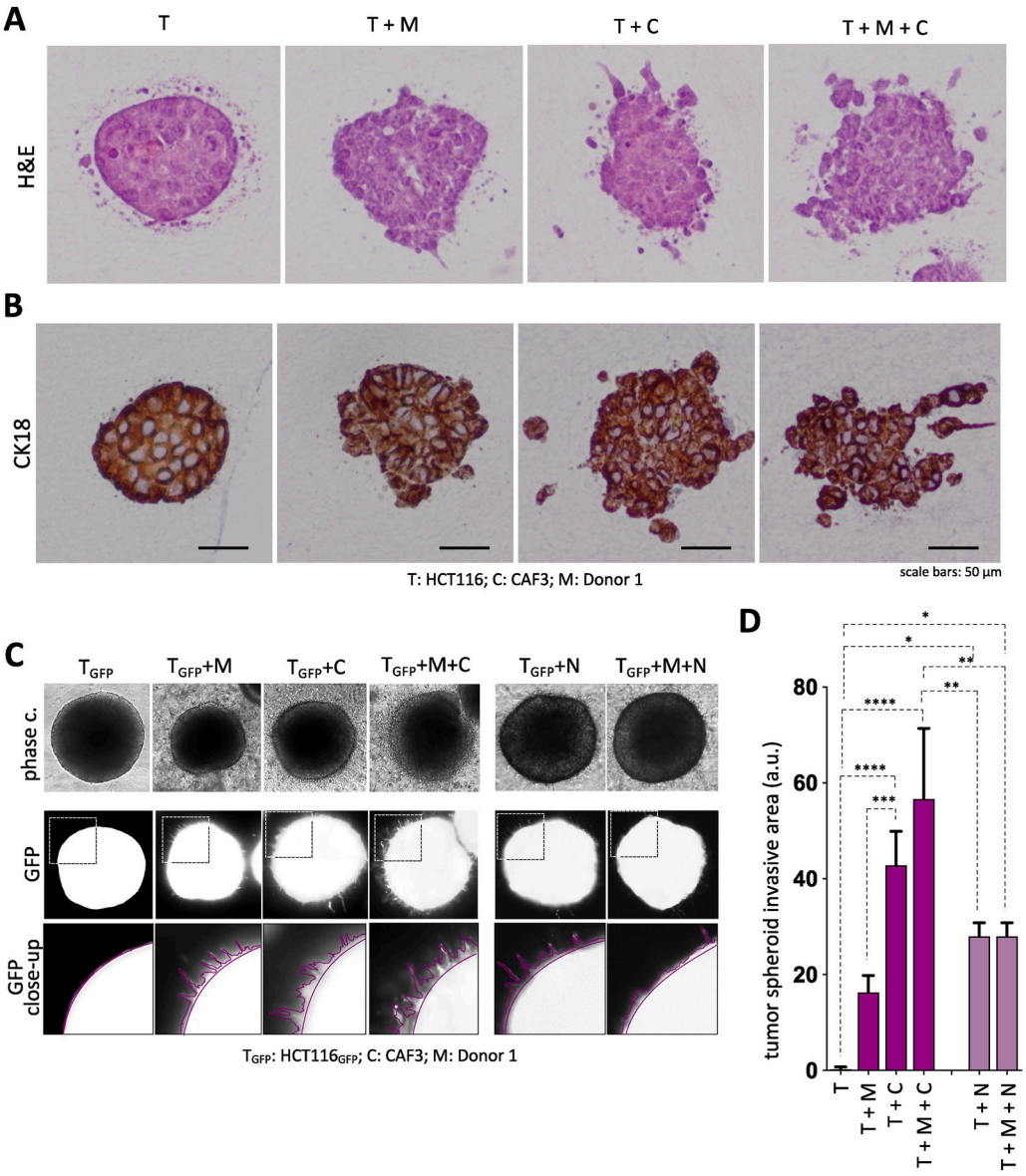

Fig. 3. ***Tumor cell invasion in collagen gel co-cultures.*** **A, B** 2×10^3 colon cancer cells (T), 2×10^5 primary fibroblasts (C or N) and 2×10^5 monocytes (giving rise to macrophages, M) were introduced into collagen I gels in mono-, double- and triple-cultures and incubated for 5 days, subjected to FFPE and sections were stained with H&E (A) or CK18 (B). **C** Spheroids were generated from HCT116-GFP cells (1500 cells/spheroid) and were incorporated into collagen gels alone and together with 2×10^5 monocyte-derived macrophages and 2×10^5 primary CAFs or 2×10^5 NAFs in co- and triple-cultures. Representative phase contrast images (top) and fluorescence images of spheroids (bottom) are shown. Invasive structures are indicated by purple lines in close-ups. **D** Invasive structures were counted and mean values of three biological replicates are shown in bar graphs. T (tumor cells, HCT116); C (CAFs, CAF3); N (normal fibroblasts, NF3) and M (macrophages). Error bars represent SEM, p-values of one-way ANOVA (Tukey's multiple comparisons) are shown. P values: *<0.05, **<0.01, ***<0.001, ****<0.0001.

macrophage-CAF interaction led to a significant rise of secreted CCL2 (Fig. 4G).

3.6. Co-culture of CAFs and macrophages significantly increase their CCL2 production, tumor cells do not express CCL2

In order to gain information on the cellular expression pattern of CCL2, triple-culture collagen gels were cultured for five days, fixed and processed for immunofluorescence confocal microscopy. Brefeldin A treatment to block secretion for 4 h prior to fixation ensured CCL2 retention in the cells. Vimentin and CD68 staining were used to distinguish the different cell types (T: $Vim^-/CD68^-$; C: $Vim^+/CD68^-$; M: $Vim^+/CD68^+$), nuclei were visualized with DAPI and the distribution of CCL2 protein was evaluated (Fig. 5A). Tumor cell clusters were completely devoid of CCL2, whereas CAFs and macrophages displayed granular CCL2 expression with a pattern resembling ER/Golgi staining (Fig. 5A and B).

Quantitative cellular CCL2 expression was assessed by flow cytometry (Fig. 5C and D) after five days of collagen gel culture. Cytokine secretion was blocked for 4 h with Brefeldin A prior to analysis. In close accordance with the ELISA data the tumor cells ($Vim^-/CD68^-$) were negative for CCL2 and did not contribute to the collective CCL2 production. CAFs ($Vim^+/CD68^-$) produced CCL2 in mono-cultures at moderate levels and showed a significant more than twofold induction when cultivated with macrophages. Macrophages ($Vim^+/CD68^+$) alone displayed very low production of CCL2, but surprisingly displayed a highly significant 40-fold induction when co-cultured with CAFs (Fig. 5E). Moreover, CD163 induction in the macrophages co-cultured with CAFs was determined in the same experiment and displayed the previously observed pattern (Fig. 5E, compare to Fig. 2B, D, E). Taken together, the appraised summed-up CCL2 production by the different cell types and their possible combinations fits to the observed amounts of CCL2 measured in the respective conditioned media by ELISA (compare to Fig. 4G).

Thus, we revealed that the interaction of CAFs with macrophages boosts CCL2 production *in vitro*, whereas the tumor cells are not involved in the release of this chemokine.

3.7. CAFs and macrophages but not tumor cells are expressing CCL2 mRNA and protein in human CRC in vivo

Many studies showed that tumor-derived CCL2 influences several

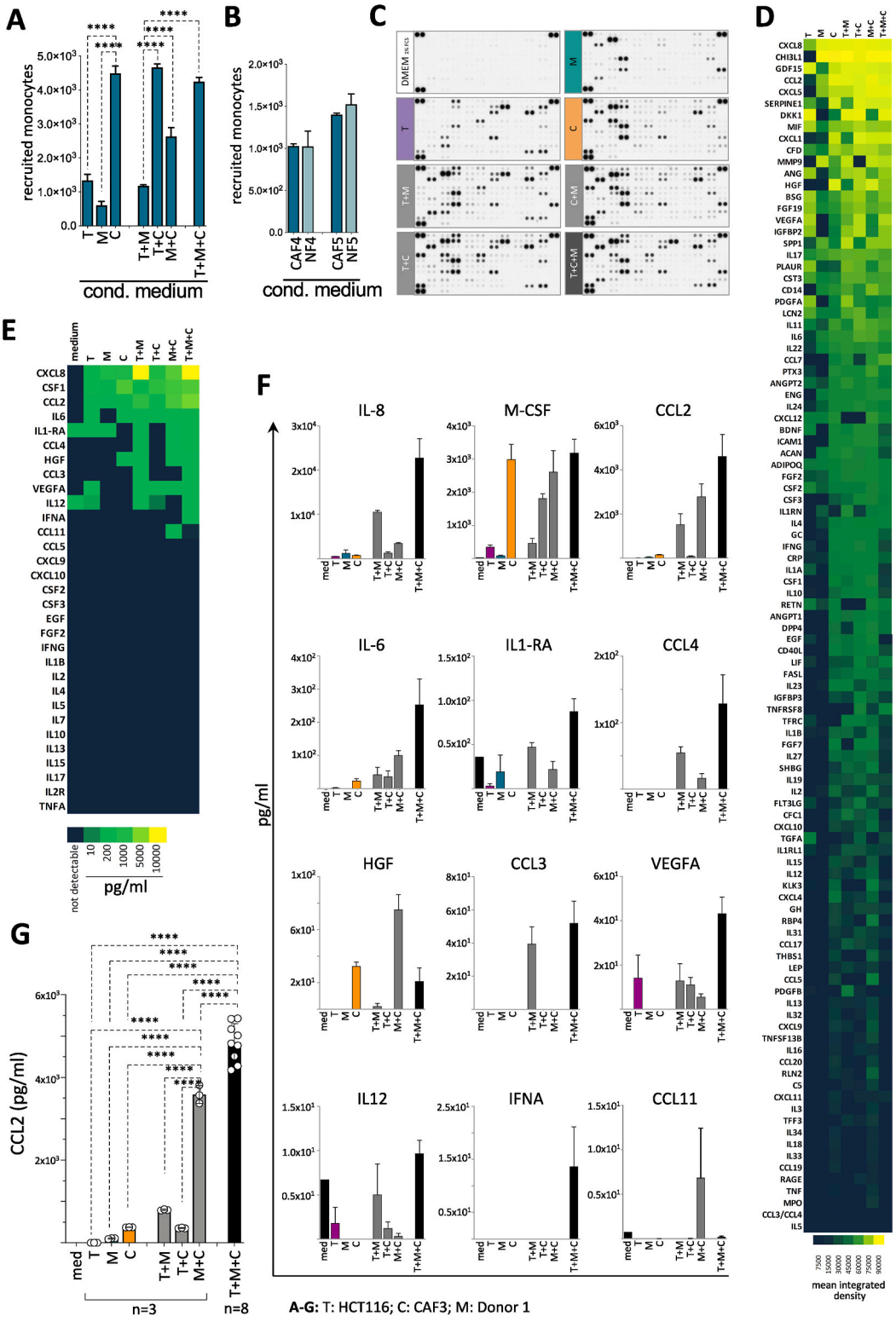

Fig. 4. ***Monocyte recruitment and cytokine profiling.*** **A**, **B** Transwell recruitment assays of monocytes towards conditioned media from CAFs macrophages and tumor cells in mono-, double-and triple cultures (A) and respective NF cultures (B). 5×10^4 monocytes (Mo) were seeded into the upper chamber of transwell inserts in serum free medium. Migrated cells in the lower chamber were stained with calcein and the fluorescence measured. **C–F** CM from mono-, double- and triple-collagen gel cultures were collected and prepared for cytokine profiling using the human cytokine XL array (C, D) and the cytokine 30-plex Luminex panel (E, F). Levels of cytokines, chemokines and growth factors are illustrated by heat maps (yellow-green- dark blue. D, E) ordered by mean protein amount from high to low. **F** Mean values of three biological replicates from the Luminex assay are shown (pg/µl). Error bars represent SEM. One way ANOVA indicated significant changes (stars). **G** Conventional CCL2 ELISA. Mean CCL2 levels (pg/ml/48 h) are shown as bars; n = 3, n = 8 for T + M + C; Error bars indicate SEM. One way ANOVA (Tukey's multiple comparisons) significance is indicated. P values: *<0.05, **<0.01, ***<0.001, ****<0.0001.

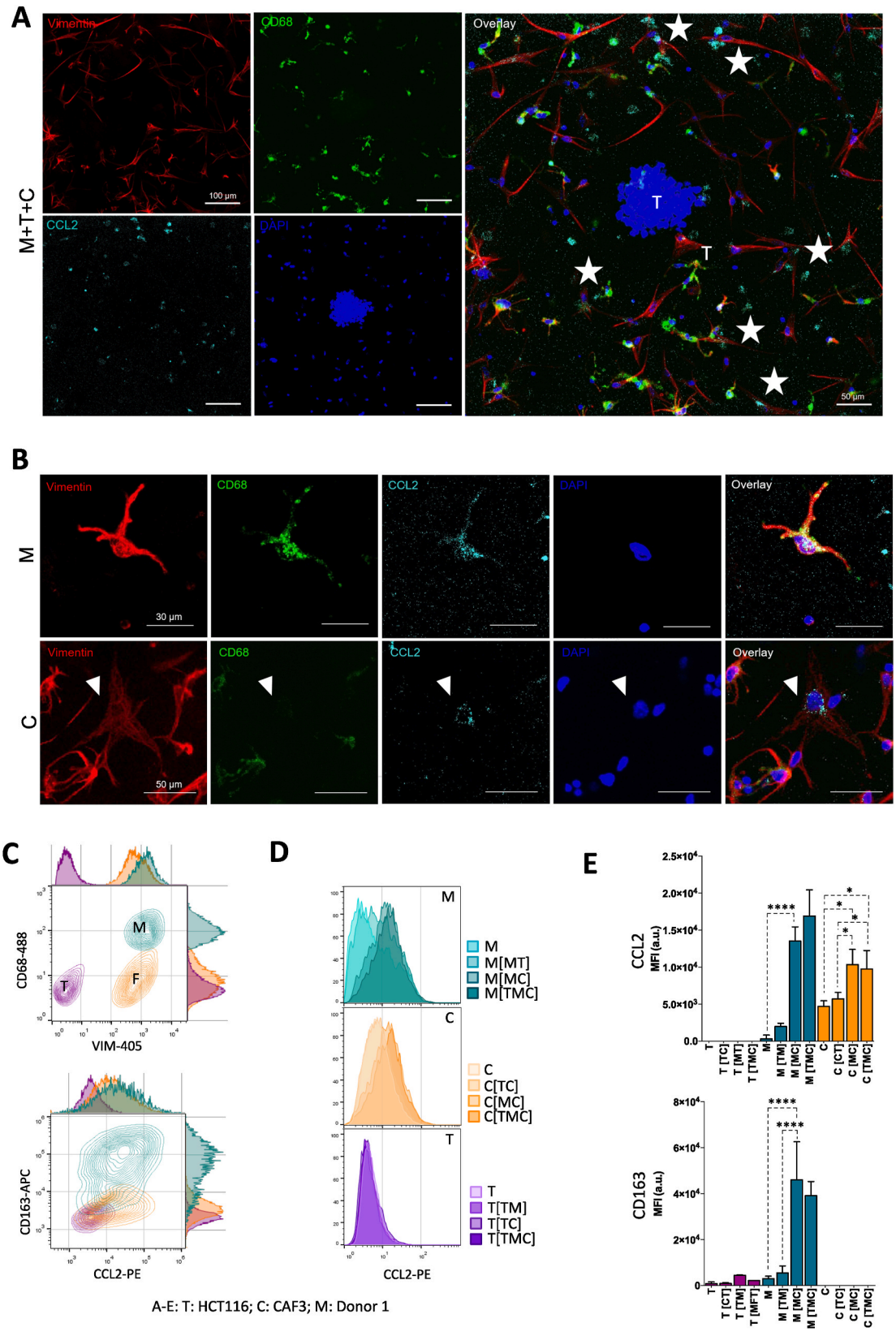

A-E: T: HCT116; C: CAF3; M: Donor 1

(caption on next page)

Fig. 5. ***CCL2 is expressed in CAFs and selectively induced in macrophages upon interaction with CAFs.*** A Representative confocal images of triple-culture collagen gels cultivated for 5 days in DMEM 2% FBS and treated with 10 μg/ml of Brefeldin A for 4 h before analysis. Macrophages (M), CAFs (C) and HCT-116 tumor cells (T) stained with Vimentin (red), CD68 (green) and CCL2 (cyan), cell nuclei were stained with DAPI (blue) are recognizable. White asterisks mark examples for cells associated with a high CCL2 expression. Note different sized scale bars. B Close-up images of one macrophage (M) or one CAF in the triple culture. White arrowheads mark the CAF and the region of high CCL2 concentration around the nucleus. Scale bars (100 μm) are indicated. C Representative flow cytometry scatter plots are depicted of HCT-116 tumor cells (T, purple), CAFs (C, orange) and macrophages (M, green) in collagen gel triple-cultures for 5 days. Vimentin-Alexa 405, CD68-Alexa 488, CCL2-PE and CD163-APC were used. D Vimentin and CD68 enabled to gate different populations and analyze the expression of CCL2 in individual cell types under mono-, co- or triple-culture. CCL2 histograms are shown for each cell type in mono-, co- and triple cultures. Depicted cell type is indicated before the square brackets and culture conditions within. As an explanatory example: T [CT]: CCL2 expression in tumor cells in co-cultures of tumor cells with CAFs. E Mean Fluorescence Intensity (MFI) of CCL2. Error bars depict SD of three measurements. Significance is indicated: ANOVA (Tukey's multiple comparisons) P values: *<0.05, **<0.01, ***<0.001, ****<0.0001.

aspects of immune cell recruitment and regulation. The term "tumor-derived" is very vague since this could either mean epithelial tumor cells but also interwoven stroma cells within the cancer tissue. We have shown that in our *in vitro* model CCL2 is clearly derived from stromal fibroblasts and macrophages. However, this might be an *in vitro* artefact. Hence, we evaluated CCL2 expression in different compartments of human colorectal cancer *in vivo* and made use of existing expression datasets of primary human colon cancer. First, analysis of the Nishida and Rupp datasets revealed that indeed CCL2 mRNA expression was significantly higher in the stromal compartment of CRC (39 patients), which was laser capture microdissected from the epithelial part (Fig. 6A). These datasets also unveiled elevated levels of CCL2 mRNA in the stroma of normal colon similar to the tumor stroma. More specifically, in the Calon dataset (6 patients) strong CCL2 expression was detectable in FAP^+ CAFs, but not in $EpCAM^+$ tumor cells, which were separated by FACS. Notably, RNA sequencing data (Isella dataset and CRRSG dataset) from 43 CRC patient-derived xenograft (PDX) models in mice displayed a similar stromal enrichment of CCL2 expression in the tumors (Fig. 6B). These data strongly support our finding of high stromal CCL2 expression by fibroblasts and macrophages. These findings were further substantiated by high CCL2 mRNA and protein expression in primary cultures of CAFs versus tumor cells (Fig. 6C). Very low CCL2 expression in 53 out of 61 CRC cell lines analyzed (Barretina [43], Garnett [44] and Wooster (unpublished) datasets; Suppl. Fig. S10) additionally validated that colon cancer cells are in general not involved in CCL2 provision.

Single cell sequencing of human colon cancers (Zhang dataset [8]) revealed similar results. Both CAF subsets (hF01 and hF02, comprising myofibroblasts and FAP^{high} cells) displayed high CCL2 expression, whereas macrophage subsets hM08, hM12, hM13 showed increased CCL2 mRNA expression. Again, epithelial cells displayed very low CCL2 expression (Fig. 6D, Suppl. Fig. S11).

To complement the previous findings, confocal immunofluorescence was performed on sections of human CRC FFPE samples to detect and quantify CCL2 along with CD68 as a marker for macrophages and DAPI as nuclear stain in four patients. Patient matched normal colon as well as tumor samples were available. We were aware that lack of Brefeldin treatment in the patients to halt CCL2 secretion might result in low CCL2 signals. However, both, in normal colon and CRC, macrophages ($CD68^+$) displaying considerable CCL2 staining (Fig. 7A) or a lack of it were detectable. This was in accordance with the single cell sequencing data of Zhang et al. [8]. Cells expressing CCL2 but not CD68 were also detectable in the stroma of normal and CRC samples. For a more quantitative analysis, stromal cells were selected on the basis of a clear DAPI staining and a categorization of these cells was performed depending on their CD68/CCL2 staining appearing around the nucleus. Macrophages displaying a CD68 to CCL2 ratio of $\geq$0.5 and $\leq$ 2.0 CCL2 were designated as macrophages expressing CCL2. Cells with a CD68/CCL2 ratio $\geq$2.0 were considered as CCL2 devoid macrophages and other stromal cells expressing CCL2 were defined by CD68/CCL2 $\leq$ 0.5. The analysis of 346 cells among healthy and tumor samples of four CRC patients revealed, according to our classification, the existence of $CCL2^+$ macrophages in both normal (Fig. 7B) and tumor (Fig. 7C) tissue samples of all patients. Moreover, macrophages lacking CCL2 and stromal cells devoid of CD68 expression but expressing were also identified. This was substantiated by co-staining of the well-established CAF marker podoplanin (PDPLN [45]) with CCL2 in the same patient cohort. Indeed, stromal cells with high PDPLN and CCL2 expression were identified alongside with $PDPLN^+/CCL2^{low}$ and $PDPLN^-/CCL2^+$ cells (Fig. 7D, Supplemental Figs. S12A and B). In contrast, alpha smooth muscle actin (SMA) positive myofibroblasts were rarely positive for CCL2 (Supplemental Figs. S12C and D).

Taken together we provide ample evidence that CCL2 expression is high in normal colon and CRC fibroblasts and in subsets of macrophages *in vitro* and *in vivo*. CCL2 is induced by macrophage-fibroblast interaction as revealed by our *in vitro* 3D assays. This CCL2 expression is restricted to stromal cells and high CCL2 expression is associated with poor prognosis in CRC as shown in the TCGA (colon adenocarcinoma) COAD overall survival analysis (Fig. 7E).

CCL2, CCR2, MCSFR as well as CD163 expression in the macrophages is dependent on active MCSFR signaling. CCL2 is induced by CCR2 inhibition suggesting a negative feedback loop.

As CCL2 displayed this interesting mode of expression and M-CSF was specifically present at high levels in CAF-containing cultures we were finally interested in interfering with the downstream signaling of the two molecules in our models.

Thus, we analyzed whether interference with CCR2 (by the specific small molecule inhibitor RS 505393) or M-CSFR signaling (by BLZ 945) might change the CAF-induced macrophage phenotype and/or CCL2 expression in the collagen gel C + M cocultures. In addition to CCL2, CD45, CD68, CD163, CCR2, M-CSFR and Vimentin levels were simultaneously assessed by flow cytometry. Cells were gated into $CD45^+/Vim^+$ macrophages and $CD45^-/Vim^+$ CAFs. Live/dead discrimination was done by Zombie staining.

As expected from published results [46], inhibition of M-CSFR signaling resulted in reduced macrophage numbers, which expressed similar amounts of CD45 (Fig. 8A and B). This, together with similar Vimentin expression irrespective of the treatment, indicated that alive macrophage populations were analyzed even under BLZ 945 treatment. High CCL2 expression in macrophages could be detected in DMSO treated CAF-myeloid cell co-cultures, validating our previous findings. Surprisingly, CCL2 expression was substantially increased when treated with the CCR2 inhibitor, and was significantly decreased to low levels equaling IgG controls when M-CSFR signaling was inhibited. CCR2 inhibition had no effect on the levels of CCR2 itself or MCSFR and CD163 expression in macrophages. However, CCR2, M-CSFR and CD163 levels dropped substantially in macrophages in M-CSFR inhibitor treated cells (Fig. 8C).

As anticipated CAFs in the co-cultures displayed high Vimentin expression with no significant differences under treatment. Also, as previously shown, we found intermediate levels of CCL2 in the CAFs in all groups without significant variation. As anticipated, CCR2, M-CSFR, CD68, CD163 and CD45 are not expressed under the various conditions (Fig. 8D).

Finally, these data could be further confirmed *in vivo* by analyzing the single cell sequencing mouse dataset of Zhang *et al.* [8]. They used mouse Renca tumors treated either with anti MCSF-R antibody (M279, Amgen [46]) or IgG controls and analyzed single cells sorted from the

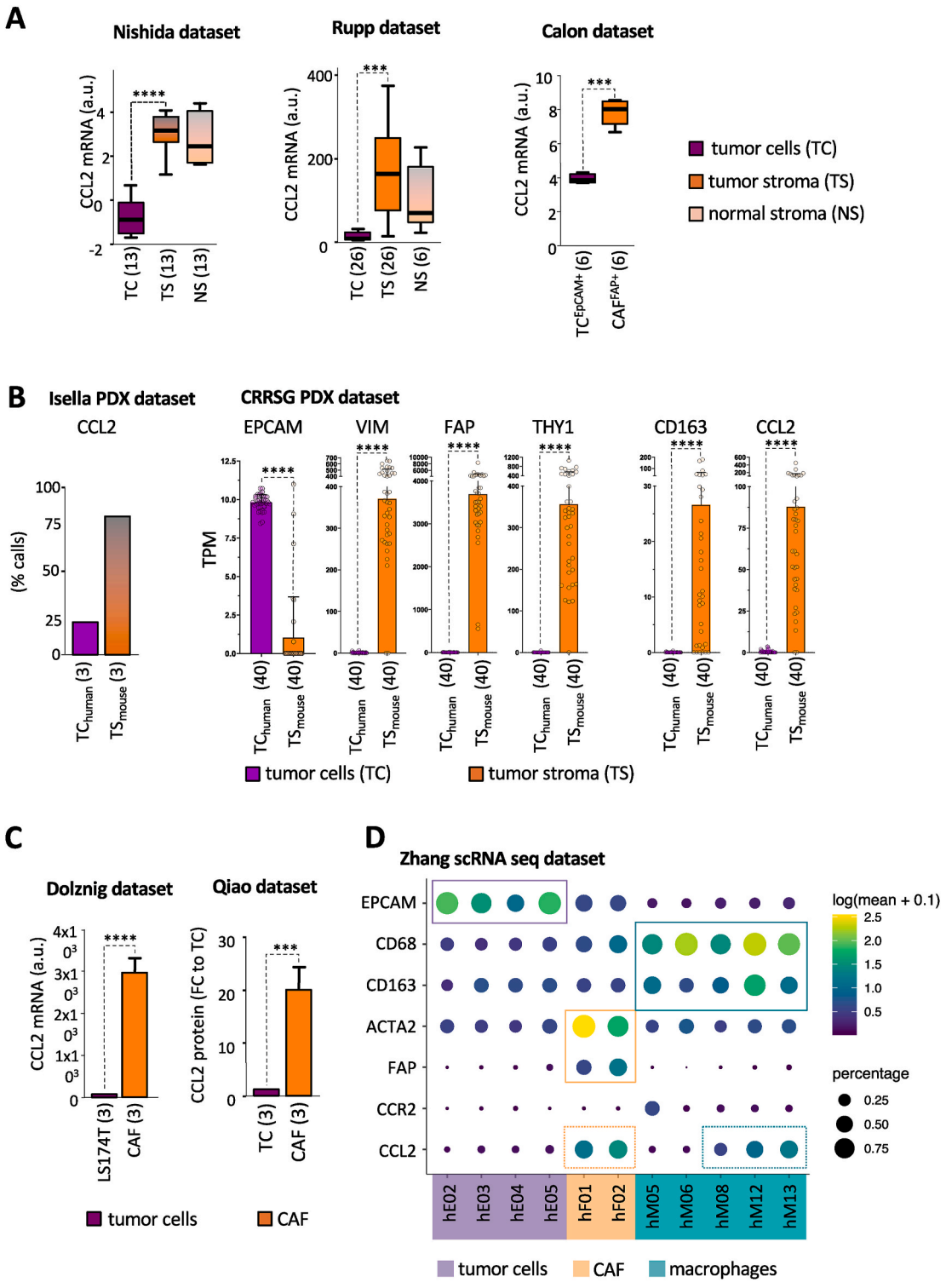

Fig. 6. ***In vivo expression of CCL2 in dissected CRC tissues, in vitro cultures and CRC single cell analysis.*** Whisker box plots (Tukey) of CCL2 mRNA expression in laser-capture-microdissected (LCM) human CRC samples: **A** Nishida dataset: tumor cells (TC, n = 13), tumor stroma (TS, n = 13), normal stroma (NS, n = 13) and Rupp data set (TC, n = 26; TS, n = 26; NS, n = 6) or Calon data set: FAC-sorted EpCAM + epithelial cells and FAP + fibroblasts (EpCAM+, n = 6; FAP+, n = 6). **B** CCL2 expression in human CRC patient derived xenograft (PDX) tumors in mice. RNA Seq data allow distinction between tumor cells (TC_{human}) and mouse stromal cells (TS_{mouse}). Percentages of mouse versus human calls for the Isella dataset (n = 3 PDX) and mean transcripts per million (TPM) for our inhouse Charles River Research Services Germany (CRRSG) dataset (n = 40 PDX). **C** Mean CCL2 mRNA and protein expression in cultivated CAFs versus tumor cells in the Dolznig (LS174T CRC cell line) and Qiao dataset (TC; SW620, HT-29, LoVo CRC cell lines), respectively. Epithelial (EpCAM), CAF (VIM, FAP, THY1) and macrophage (CD163) markers are shown as controls. Error bars are SD. Student's T-test P values are indicated. P values: *<0.05, **<0.01, ***<0.001, ****<0.0001. **D** Mean gene expression (color) and percentage of expressed cells (dot size) in selected clusters of the Zhang scRNA Seq dataset ("hF01","hF02", "hM05", "hM06", "hM08", "hM12", "hM13", "hE02", "hE03", "hE04", "hE05") were graphed. A total of 2003 cells were shown (clusters contained between 58 and 544 cells).

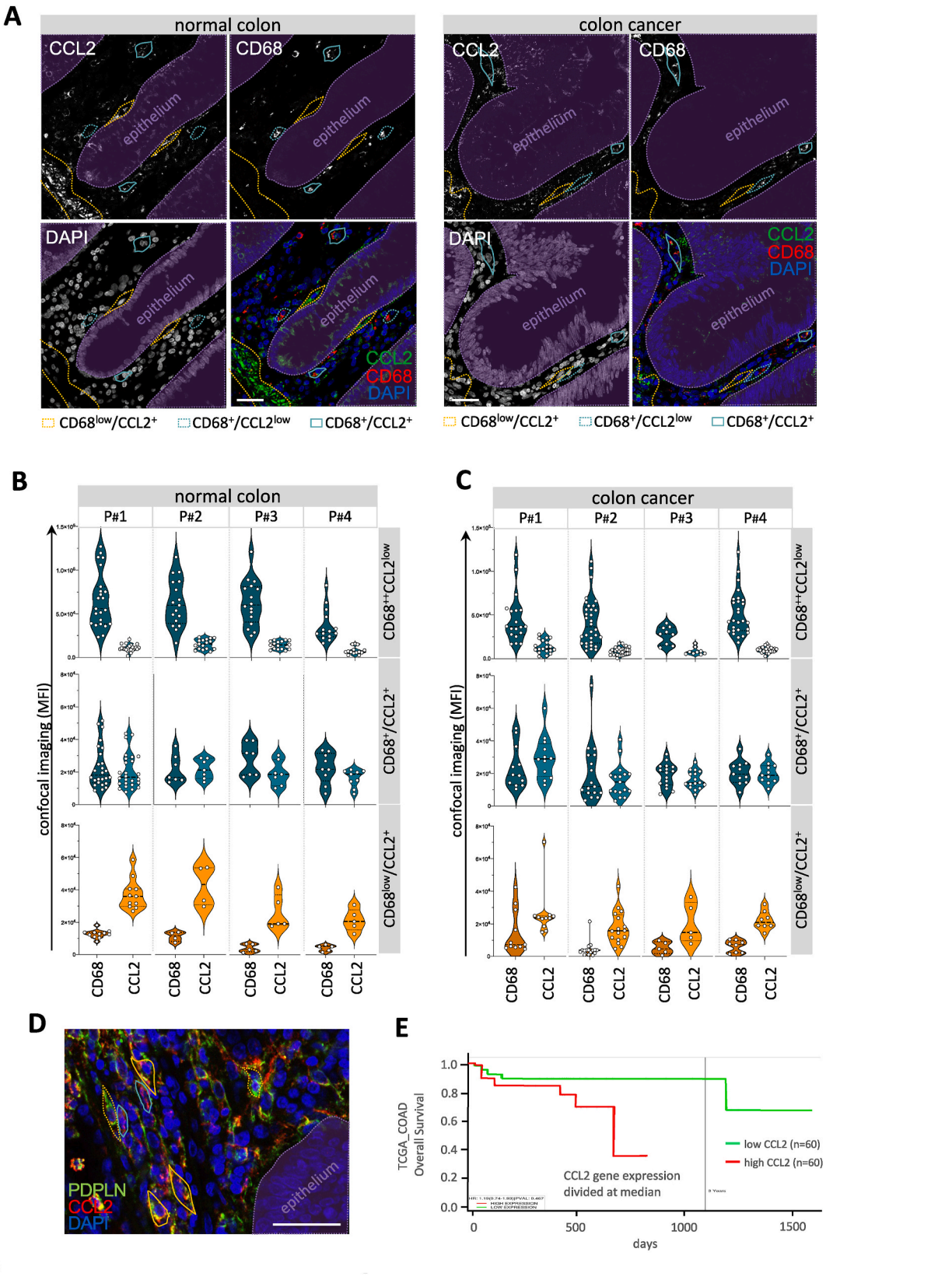

(caption on next page)

Fig. 7. ***CCL2 mean expression in stromal cells and macrophages in CRC.*** A Sections of normal and CRC FFPE samples from four patients were immunofluorescently stained for CD68 (red) and CCL2 (green) and DAPI (nuclei, blue). Representative individual stains are shown in greyscale and as color merge. Epithelial structures (purple overlay) were excluded from analysis. Encircled cells are examples of either $CCL2^+$ stromal cells (orange dotted outlines), or $CD68^+$ macrophages (turquoise dotted or continuous outlines) expressing or lacking CCL2 expression. B, C Violin plots indicating the MFI of CD68 and CCL2 expression in four normal colon samples and the corresponding tumor samples are shown per patient (P#1–4). A total of 346 cells were analyzed and categorized as follows: stromal cells expressing CCL2: [(CD68/CCL2) $\leq$ 0.5]; macrophages expressing CCL2: [0.5 $\leq$ (CD68/CCL2) $\leq$ 2.0]; macrophages expressing low or no CCL2: [(CD68/CCL2) $\geq$ 2.0]. Dots indicate individual cells analyzed. Stromal cells are indicated in orange, macrophages in green. D Immunofluorescence analysis of CCL2 (red) and podoplanin (PDPLN, green) in a CRC patient sample; nuclei are in blue (DAPI), epithelial structures overlayed in purple. Encircled cells are examples of either $PDPLN^{+/}CCL2^{low}$ CAFs (orange dotted outlines), $PDPLN^{+/}CCL2^{+}$ CAFs (orange outlines) or $PDPLN^{-/}CCL2^{+}$ cells (turquoise outlines). All scale bars: 50 μm. E Survival analysis of 120 CRC patients using the TCGA COAD dataset. Data were bifurcated for high and low CCL2 expression at the median and a Kaplan–Meier survival plot was generated with the SurvExpress online tool [68]. Red, high; green, low expression of CCL2.

tumors. CCR2 inhibition was not performed in this study. However, they show that anti M-CSFR treatment reduced the number of myeloid cells in the tumor, supporting our finding in the *in vitro* model (compare Fig. 8A). Moreover, in certain subsets of macrophages (mM11, mM12) the treatment also reduced CCL2, CCR2 and CD163 expression (Fig. 8E, Suppl. Fig. S13) in perfect agreement with our *in vitro* data.

In summary, we revealed dynamic regulation of the macrophage phenotype by M-CSFR signaling in the myeloid cells activated by CAF-derived MCSF, whereas CCR2 inhibition resulted in a – probably feed forward – compensatory increase of CCL2 expression in the macrophages. We show compelling evidence that our novel 3D co-culture systems recapitulate *in vivo* like responses and provide human model systems for functional testing and interference.

4. Discussion

Macrophages are highly phagocytic myeloid cells, which also display antigen presentation and secretory features thereby contributing to both innate and adaptive immune responses. The normal colon is one of the organs displaying highest macrophage density [47]. Moreover, macrophages in the colon display a rapid turnover time of a few weeks [5], and are continuously replenished by recruitment of circulating monocytes [3,4] and their site-specific differentiation and functional polarization, being unique to this organ. Under homeostatic conditions, colonic macrophages display an immunosuppressive, pro-tolerogenic phenotype, which is characterized by high CD163, CD206 and CD68 expression [1].

If looking at histological sections of normal human colon and CRC, it is evident that TAMs predominantly reside in the stroma and are rarely seen directly infiltrating the tumor epithelium [13]. Thus, one can conclude that recruitment of monocytes, their retainment and differentiation to macrophages and their functional polarization is predominantly dependent on cues derived from stromal cells within normal intestinal tissue and cancer. Indeed, we identify normal fibroblasts and CAFs to be major players in these processes and that tumor epithelial cells obviously play a minor role.

First, we clearly demonstrate that a $CD68^{high}/CD163^{high}$ macrophage phenotype, reminiscent of the gut macrophage phenotype under homeostatic conditions, is established by the interaction of monocytes or M-CSF predifferentiated monocyte-derived macrophages (MDM) with CAFs or NFs, which is independent of cancer cells. Monocyte infiltration and subsequent differentiation to TAMs in colon cancer was shown *in vivo* by scRNA sequencing experiments using RNA velocity analyses [8]. Even predifferentiated inflammatory MDMs ($M_{LPS/IFN\gamma}$) are reprogrammed by CAFs or CAFs + tumor cells (see Fig. 2E) to express high levels of CD163, indicating a dominant effect of the CAFs independent of the source of the NFs, CAFs, tumor cells or monocytes. This is in accordance with the well-established idea that the normal mucosal macrophages and the majority of colonic TAMs display an anti-inflammatory phenotype in advanced cancers [48,49]. Moreover, colonic CAFs have already been described to shape an M2-like phenotype in macrophages *in vitro* [50]. There is growing evidence from scRNA sequencing that either a continuum or distinct TAM subtypes exist in different cancers, however these do not fit the simplified bipartite M1/M2 model [7–9]. Whether CAFs in our 3D organotypic assays are preferentially supporting one of the two identified TAM subtypes in CRC, or is associated with both, needs to be addressed in the future.

Interestingly, as discussed above, polarization to the $CD163^{high}$ macrophage phenotype is supported by both, NF and CAF, however, there is a significant difference in tumor cell invasion depending on the fibroblast phenotype. The invasive promoting effect of CAFs on cancer cells is well established [51], however less is known about the impact on cancer cell invasion upon the interaction with macrophages and CAFs. In line with published results [27], tumor cells co-cultured with CAFs displayed elevated invasive potential as compared to the TC/NF pairs. Interestingly this invasive potential was further significantly increased by the presence of macrophages. This was not the case in NF/M co-cultures. Indeed, our findings are supported by reports demonstrating that CAF-educated TAMs can increase the migratory potential of CRC lines [50,52]. Hence, we conclude that CAFs might preserve the intrinsic function of colonic NFs to differentiate and polarize monocytes to anti-inflammatory macrophages as in normal gut homeostasis but gain the property to elevate cancer cell invasion alone and in concert with TAMs. A similar finding has been reported in an encapsulated 3D lung cancer model consisting of CAFs, tumor cells and monocytes [53].

It is also evident from our 3D co-culture experiments that conditioned media from cultures containing NFs or CAFs was most potent to induce monocyte attraction, whereas tumor cells alone or macrophages or their co-cultures were not very efficient (see Fig. 4A and Supplemental Fig. S9). This suggests that again stromal fibroblasts produce the major cytokines and chemokines to ensure efficient monocyte recruitment. Cytokine profiling did not reveal a single factor recapitulating the pattern of recruitment thus we conclude that a mixture of chemokines might be responsible. Actually, many factors, which were detectable at high levels and displayed cell or co-culture specific patterns, are essential or take part in monocyte recruitment, such as CCL2 [54], CXCL12 [55], M-CSF [46], IL8 [50]. Cytokine array and bead ELISAs clearly display interesting patterns of M-CSF and CCL2 expression amongst others. M-CSF was exclusively produced by CAFs in the cultures and showed almost no variation in co-cultures containing CAFs, whereas CCL2 was only secreted at low levels in CAF monocultures and selectively induced in CAF-macrophage co-cultures and to a lesser extend in tumor cell -macrophage cocultures. As these two factors are crucial for monocyte recruitment, survival and differentiation we focused our further analysis on them.

Using our co-cultures, we clearly demonstrate here, by analyzing expression data of dissected CRC patient material or scRNA sequencing, that CCL2 is predominantly expressed in stromal fibroblasts and in macrophages in human CRC both *in vitro* and *in vivo*, whereas tumor epithelial cells do not express it. CCL2 expression was also reported, in breast cancer stroma [56,57], in lung and skin fibroblasts [58], in hepatic myofibroblasts [59], colonic CAFs [60] as well as in bone-marrow-derived mesenchymal stromal cells [61]. Moreover, proteome profiling of cultivated CRC fibroblasts also showed CCL2 expression and secretion [62]. Thus, our results and data from literature strongly support the notion that fibroblasts in homeostasis and cancer are major producers of CCL2.

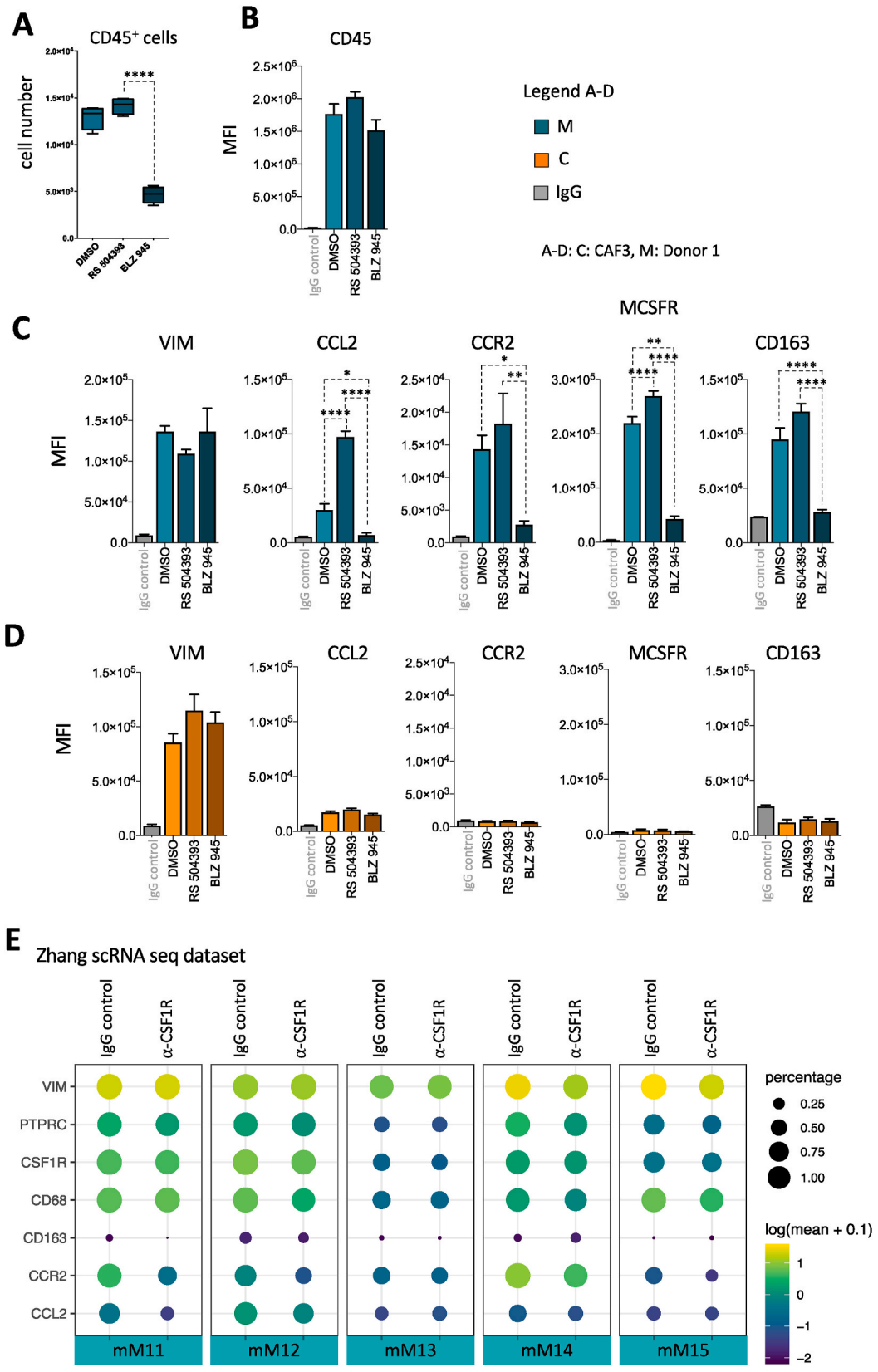

Fig. 8. Effects of CCR2 and M-CSFR inhibition on macrophage phenotypes. 3×10^5 M_{MCSF} were embedded in collagen gels with 3×10^5 CAFs and treated with either DMSO, CCR2 small molecule inhibitor RS 504393 (2 μM) or M-CSFR small molecule inhibitor BLZ 945 (1 μM) for six days (media and factor refresh every 48 h). **A** Mean cell number of $CD45^+$ cells (i.e. macrophages) per 4×10^4 total single cells analyzed. **B, C** MFI is shown for CD45, CCR2; M-CSFR; CD163 (n = 3) in macrophages and **D** in CAFs. IgG-controls are indicated. Error bars show the SEM and significances are illustrated (one way ANOVA; Tukey's multiple comparisons). P values: *<0.05, **<0.01, ***<0.001, ****<0.0001. **E** Mean gene expression (color) and percentage of expressed cells (dot size) in macrophage clusters of the mouse Renca colon cancer treated with anti-CSF1R or IgG control (Zhang scRNA Seq dataset) were graphed. PTPRC: CD45.

Of note, the modular nature of our co-culture assays revealed a strong and selective induction of CCL2 expression in the MDMs, when CAFs were present. Thus, we discovered a novel mode of CCL2 regulation where CAFs induced CCL2 production in the macrophages thereby possibly ensuring efficient recruitment of monocytes. High CCL2 levels in macrophages were also confirmed in distinct macrophage subsets in human and mouse tumors *in vivo* by scRNA analysis (see Figs. 6 and 8) and immunofluorescence (Fig. 7). This strongly underscores our *in vitro* data and is further supported by reported CCL2 expression in mouse macrophages during inflammation [24,63], in a xenograft breast cancer model and in TAMs of human mammary tumors [56].

As CCL2 and M-CSF displayed an interesting expression pattern and both molecules or their downstream signaling are considered as promising targets in immunotherapy [19], we finally investigated the impact of their selective inhibition. CCL2/CCR2 inhibition is effective to reduce monocyte release from the bone marrow and to inhibit recruitment but may also interfere with myeloid cell function [42,64]. Hence, we were interested whether fibroblast-derived CCL2 and subsequent CCL2 production by macrophages in the co-cultures had an effect on the macrophage phenotype in the cultures. Unexpectedly, macrophages significantly increased CCL2 expression under CCR2 blockade, suggesting a negative feedback loop of active CCR2 signaling on the CCL2 production in the cells (Fig. 8C). Of note, other markers like CCR2, CD168 or MCSFR did not change, which implicates a specific effect on the CCL2/CCR2 cascade but not on the general macrophage phenotype *per se*. In contrast, blocking MCSFR substantially reduced macrophage number in the cultures which showed decreased CCL2, CCR2, MCSFR and CD163 expression. The loss of macrophages could be due to cell death, as the survival of these cells may depend on M-CSFR signaling. The remaining cells however, could be a distinct sub-population of macrophages and thus do not necessary represents the total population of the macrophage in the assay and or in the tumor. The reduction in cell number is in accordance with the fact that inhibition of M-CSF affects myeloid cell survival, differentiation and function [65] ultimately leading to substantial TAM reduction in cancers. Indeed, the depletion of CD68/CD163 positive macrophages in solid tumors was described in a Phase I study using emactuzumab targeting CSF1R [66]. However, in mice certain TAM subsets survive under M-CSFR inhibitor treatment as shown by the resistance of some macrophage subtypes (mM11/13/15, see Fig. 8E) [8]. Since roughly one third of the macrophages were still present under MSCFR inhibition in our cultures, it is tempting to speculate that these might represent resistant ones. They might be similar to those resistant macrophages which were identified by Zhang and colleagues [8]. This has to be further evaluated in the future by gene expression analysis and marker examination. The CCL2/CCR2 and the M-CSF/CSF1R signaling axes are important candidates for immunotherapeutic intervention in cancer and clinical tolerability is well documented already, however, preclinical data urge for the use of combinatorial therapies [67], which are currently evaluated [2] but still need improved biological knowledge, e.g., for proper patient stratification or inhibitor combinations. We are confident that our novel model can contribute to this task.

Taken together, we have established a promising preclinical CRC model to investigate myeloid cell phenotypes and function in the context of complex tumor-stroma interaction. We provide clear evidence that colonic fibroblasts are major components for monocyte recruitment/differentiation and macrophage survival/polarization. This assay has the potential to be expanded on other immune cells, such as T cell function, and essentially contribute to the better understanding of cancer biology and immunology and is suitable to test and biologically evaluate (immunomodulating) anti-cancer drugs.

Author contributions

Mira Stadler: Methodology, Validation, Formal analysis, Investigation, Visualization, Karoline Pudelko: Methodology, Validation, Formal analysis, Investigation, Visualization, Alexander Biermeier: Methodology, Validation, Formal analysis, Investigation, Visualization, Natalie Walterskirchen: Methodology, Validation, Formal analysis, Investigation, Visualization, Funding acquisition, Anthoula Gaigneaux: Formal analysis, Investigation, Data curation, Visualization, Claudia Weindorfer: Formal analysis, Investigation, Nathalie Harrer: Investigation, Hagen Klett: Formal analysis, Data curation, Markus Hengstschläger: Writing – review & editing, Funding acquisition, Julia Schüler: Project administration, Wolfgang Sommergruber: Formal analysis, Writing – review & editing, Supervision, Rudolf Oehler: Writing – review & editing, Supervision, Michael Bergmann: Formal analysis, Writing – review & editing, Elisabeth Letellier: Writing – review & editing, Visualization, Supervision, Project administration, Funding acquisition Helmut Dolznig: Conceptualization, Methodology, Validation, Formal analysis, Investigation, Writing – original draft, Visualization, Supervision, Project administration, Funding acquisition

Declaration of competing interest

The authors declare no conflict of interest.

Acknowledgements

HD is supported by the EU (SECRET-ITN 859962) and the Niederösterreichische Forschungs-und Bildungsges. m.bH. (NFB, LSC18-017); NW is supported by the Austrian Research Promotion Agency (FFG; 868039), EL is supported by the Luxembourg National Research Fund [CORE/C16/BM/11282028, PoC/18/12554295, the Fondation Marie-Jeanne and Edmond Schumacher, the Fondation Gustave and Simone Prévot.

Appendix A. Supplementary data

Supplementary data to this article can be found online at https://doi.org/10.1016/j.canlet.2021.07.006.

References

[1] E. Gonzalez-Dominguez, R. Samaniego, J.L. Flores-Sevilla, S.F. Campos-Campos, G. Gomez-Campos, A. Salas, et al., CD163L1 and CLEC5A discriminate subsets of human resident and inflammatory macrophages in vivo, J. Leukoc. Biol. 98 (4) (2015) 453–466.
[2] D.G. DeNardo, B. Ruffell, Macrophages as regulators of tumour immunity and immunotherapy, Nat. Rev. Immunol. 19 (6) (2019) 369–382.
[3] S. Yona, K.W. Kim, Y. Wolf, A. Mildner, D. Varol, M. Breker, et al., Fate mapping reveals origins and dynamics of monocytes and tissue macrophages under homeostasis, Immunity 38 (1) (2013) 79–91.
[4] C.C. Bain, C.L. Scott, H. Uronen-Hansson, S. Gudjonsson, O. Jansson, O. Grip, et al., Resident and pro-inflammatory macrophages in the colon represent alternative context-dependent fates of the same Ly6Chi monocyte precursors, Mucosal Immunol. 6 (3) (2013) 498–510.
[5] A. Rivollier, J. He, A. Kole, V. Valatas, B.L. Kelsall, Inflammation switches the differentiation program of Ly6Chi monocytes from antiinflammatory macrophages to inflammatory dendritic cells in the colon, J. Exp. Med. 209 (1) (2012) 139–155.
[6] C.C. Bain, A. Schridde, Origin, differentiation, and function of intestinal macrophages, Front. Immunol. 9 (2018) 2733.
[7] E. Azizi, A.J. Carr, G. Plitas, A.E. Cornish, C. Konopacki, S. Prabhakaran, et al., Single-cell map of diverse immune phenotypes in the breast tumor microenvironment, Cell 174 (5) (2018) 1293–1308 e36.
[8] L. Zhang, Z. Li, K.M. Skrzypczynska, Q. Fang, W. Zhang, S.A. O'Brien, et al., Single-cell analyses inform mechanisms of myeloid-targeted therapies in colon cancer, Cell 181 (2) (2020) 442–459 e29.
[9] S. Muller, G. Kohanbash, S.J. Liu, B. Alvarado, D. Carrera, A. Bhaduri, et al., Single-cell profiling of human gliomas reveals macrophage ontogeny as a basis for regional differences in macrophage activation in the tumor microenvironment, Genome Biol. 18 (1) (2017) 234.
[10] R.L. Siegel, K.D. Miller, A. Goding Sauer, S.A. Fedewa, L.F. Butterly, J.C. Anderson, et al., Colorectal cancer statistics, 2020, CA A Cancer J. Clin. 70 (3) (2020) 145–164.
[11] C. Isella, A. Terrasi, S.E. Bellomo, C. Petti, G. Galatola, A. Muratore, et al., Stromal contribution to the colorectal cancer transcriptome, Nat. Genet. 47 (4) (2015) 312–319.

[12] A. Calon, E. Lonardo, A. Berenguer-Llergo, E. Espinet, X. Hernando-Momblona, M. Iglesias, et al., Stromal gene expression defines poor-prognosis subtypes in colorectal cancer, Nat. Genet. 47 (4) (2015) 320–329.
[13] K. Strasser, H. Birnleitner, A. Beer, D. Pils, M.C. Gerner, K.G. Schmetterer, et al., Immunological differences between colorectal cancer and normal mucosa uncover a prognostically relevant immune cell profile, OncoImmunology 8 (2) (2019) e1537693.
[14] Y. Nakayama, N. Nagashima, N. Minagawa, Y. Inoue, T. Katsuki, K. Onitsuka, et al., Relationships between tumor-associated macrophages and clinicopathological factors in patients with colorectal cancer, Anticancer Res. 22 (6C) (2002) 4291–4296.
[15] J. Forssell, A. Oberg, M.L. Henriksson, R. Stenling, A. Jung, R. Palmqvist, High macrophage infiltration along the tumor front correlates with improved survival in colon cancer, Clin. Canc. Res. 13 (5) (2007) 1472–1479.
[16] Q.W. Zhang, L. Liu, C.Y. Gong, H.S. Shi, Y.H. Zeng, X.Z. Wang, et al., Prognostic significance of tumor-associated macrophages in solid tumor: a meta-analysis of the literature, PloS One 7 (12) (2012) e50946.
[17] L. Ye, T. Zhang, Z. Kang, G. Guo, Y. Sun, K. Lin, et al., Tumor-infiltrating immune cells act as a marker for prognosis in colorectal cancer, Front. Immunol. 10 (2019) 2368.
[18] C. Yang, C. Wei, S. Wang, D. Shi, C. Zhang, X. Lin, et al., Elevated cd163(+)/CD68(+) ratio at tumor invasive front is closely associated with aggressive phenotype and poor prognosis in colorectal cancer, Int. J. Biol. Sci. 15 (5) (2019) 984–998.
[19] S. Edin, M.L. Wikberg, A.M. Dahlin, J. Rutegard, A. Oberg, P.A. Oldenborg, et al., The distribution of macrophages with a M1 or M2 phenotype in relation to prognosis and the molecular characteristics of colorectal cancer, PloS One 7 (10) (2012) e47045.
[20] O. Canli, A.M. Nicolas, J. Gupta, F. Finkelmeier, O. Goncharova, M. Pesic, et al., Myeloid cell-derived reactive oxygen species induce epithelial mutagenesis, Canc. Cell 32 (6) (2017) 869–883 e5.
[21] L. Deng, J.F. Zhou, R.S. Sellers, J.F. Li, A.V. Nguyen, Y. Wang, et al., A novel mouse model of inflammatory bowel disease links mammalian target of rapamycin-dependent hyperproliferation of colonic epithelium to inflammation-associated tumorigenesis, Am. J. Pathol. 176 (2) (2010) 952–967.
[22] L. Zhao, S.Y. Lim, A.N. Gordon-Weeks, T.T. Tapmeier, J.H. Im, Y. Cao, et al., Recruitment of a myeloid cell subset (CD11b/Gr1 mid) via CCL2/CCR2 promotes the development of colorectal cancer liver metastasis, Hepatology 57 (2) (2013) 829–839.
[23] E.R. Stanley, V. Chitu, CSF-1 receptor signaling in myeloid cells, Cold Spring Harb Perspect Biol 6 (6) (2014).
[24] B.K. Popivanova, F.I. Kostadinova, K. Furuichi, M.M. Shamekh, T. Kondo, T. Wada, et al., Blockade of a chemokine, CCL2, reduces chronic colitis-associated carcinogenesis in mice, Canc. Res. 69 (19) (2009) 7884–7892.
[25] B. Mroczko, M. Groblewska, U. Wereszczynska-Siemiatkowska, B. Okulczyk, B. Kedra, W. Laszewicz, et al., Serum macrophage-colony stimulating factor levels in colorectal cancer patients correlate with lymph node metastasis and poor prognosis, Clin. Chim. Acta 380 (1–2) (2007) 208–212.
[26] A. Mantovani, A. Sica, Macrophages, innate immunity and cancer: balance, tolerance, and diversity, Curr. Opin. Immunol. 22 (2) (2010) 231–237.
[27] H. Dolznig, C. Rupp, C. Puri, C. Haslinger, N. Schweifer, E. Wieser, et al., Modeling colon adenocarcinomas in vitro a 3D co-culture system induces cancer-relevant pathways upon tumor cell and stromal fibroblast interaction, Am. J. Pathol. 179 (1) (2011) 487–501.
[28] C. Unger, N. Kramer, D. Unterleuthner, M. Scherzer, A. Burian, A. Rudisch, et al., Stromal-derived IGF2 promotes colon cancer progression via paracrine and autocrine mechanisms, Oncogene 36 (38) (2017) 5341–5355.
[29] C. Rupp, M. Scherzer, A. Rudisch, C. Unger, C. Haslinger, N. Schweifer, et al., IGFBP7, a novel tumor stroma marker, with growth-promoting effects in colon cancer through a paracrine tumor-stroma interaction, Oncogene 34 (7) (2015) 815–825.
[30] N. Nishida, M. Nagahara, T. Sato, K. Mimori, T. Sudo, F. Tanaka, et al., Microarray analysis of colorectal cancer stromal tissue reveals upregulation of two oncogenic miRNA clusters, Clin. Canc. Res. 18 (11) (2012) 3054–3070.
[31] J. Qiao, C.Y. Fang, S.X. Chen, X.Q. Wang, S.J. Cui, X.H. Liu, et al., Stroma derived COL6A3 is a potential prognosis marker of colorectal carcinoma revealed by quantitative proteomics, Oncotarget 6 (30) (2015) 29929–29946.
[32] T. Conway, J. Wazny, A. Bromage, M. Tymms, D. Sooraj, E.D. Williams, et al., Xenome–a tool for classifying reads from xenograft samples, Bioinformatics 28 (12) (2012) i172–i178.
[33] D. Kim, J.M. Paggi, C. Park, C. Bennett, S.L. Salzberg, Graph-based genome alignment and genotyping with HISAT2 and HISAT-genotype, Nat. Biotechnol. 37 (8) (2019) 907–915.
[34] M. Pertea, G.M. Pertea, C.M. Antonescu, T.C. Chang, J.T. Mendell, S.L. Salzberg, StringTie enables improved reconstruction of a transcriptome from RNA-seq reads, Nat. Biotechnol. 33 (3) (2015) 290–295.
[35] R.C.R. Team, A language and environment for statistical computing [Available from: https://www.R-project.org/, 2020.
[36] W. Huber, V.J. Carey, R. Gentleman, S. Anders, M. Carlson, B.S. Carvalho, et al., Orchestrating high-throughput genomic analysis with Bioconductor, Nat. Methods 12 (2) (2015) 115–121.
[37] J. Cao, M. Spielmann, X. Qiu, X. Huang, D.M. Ibrahim, A.J. Hill, et al., The single-cell transcriptional landscape of mammalian organogenesis, Nature 566 (7745) (2019) 496–502.
[38] X. Qiu, Q. Mao, Y. Tang, L. Wang, R. Chawla, H.A. Pliner, et al., Reversed graph embedding resolves complex single-cell trajectories, Nat. Methods 14 (10) (2017) 979–982.
[39] C. Trapnell, D. Cacchiarelli, J. Grimsby, P. Pokharel, S. Li, M. Morse, et al., The dynamics and regulators of cell fate decisions are revealed by pseudotemporal ordering of single cells, Nat. Biotechnol. 32 (4) (2014) 381–386.
[40] A. Rudisch, M.R. Dewhurst, L.G. Horga, N. Kramer, N. Harrer, M. Dong, et al., High EMT signature score of invasive non-small cell lung cancer (NSCLC) cells correlates with NFkappaB driven colony-stimulating factor 2 (CSF2/GM-CSF) secretion by neighboring stromal fibroblasts, PloS One 10 (4) (2015) e0124283.
[41] N. Eiro, L. Gonzalez, A. Martinez-Ordonez, B. Fernandez-Garcia, L.O. Gonzalez, S. Cid, et al., Cancer-associated fibroblasts affect breast cancer cell gene expression, invasion and angiogenesis, Cell. Oncol. 41 (4) (2018) 369–378.
[42] M. Gschwandtner, R. Derler, K.S. Midwood, More than just attractive: how CCL2 influences myeloid cell behavior beyond chemotaxis, Front. Immunol. 10 (2019) 2759.
[43] J. Barretina, G. Caponigro, N. Stransky, K. Venkatesan, A.A. Margolin, S. Kim, et al., The Cancer Cell Line Encyclopedia enables predictive modelling of anticancer drug sensitivity, Nature 483 (7391) (2012) 603–607.
[44] M.J. Garnett, E.J. Edelman, S.J. Heidorn, C.D. Greenman, A. Dastur, K.W. Lau, et al., Systematic identification of genomic markers of drug sensitivity in cancer cells, Nature 483 (7391) (2012) 570–575.
[45] S.Y. Choi, R. Sung, S.J. Lee, T.G. Lee, N. Kim, S.M. Yoon, et al., Podoplanin, alpha-smooth muscle actin or S100A4 expressing cancer-associated fibroblasts are associated with different prognosis in colorectal cancers, J. Kor. Med. Sci. 28 (9) (2013) 1293–1301.
[46] K.P. MacDonald, J.S. Palmer, S. Cronau, E. Seppanen, S. Olver, N.C. Raffelt, et al., An antibody against the colony-stimulating factor 1 receptor depletes the resident subset of monocytes and tissue- and tumor-associated macrophages but does not inhibit inflammation, Blood 116 (19) (2010) 3955–3963.
[47] S.H. Lee, P.M. Starkey, S. Gordon, Quantitative analysis of total macrophage content in adult mouse tissues. Immunochemical studies with monoclonal antibody F4/80, J. Exp. Med. 161 (3) (1985) 475–489.
[48] A. Sica, A. Mantovani, Macrophage plasticity and polarization: in vivo veritas, J. Clin. Invest. 122 (3) (2012) 787–795.
[49] G. Solinas, G. Germano, A. Mantovani, P. Allavena, Tumor-associated macrophages (TAM) as major players of the cancer-related inflammation, J. Leukoc. Biol. 86 (5) (2009) 1065–1073.
[50] R. Zhang, F. Qi, F. Zhao, G. Li, S. Shao, X. Zhang, et al., Cancer-associated fibroblasts enhance tumor-associated macrophages enrichment and suppress NK cells function in colorectal cancer, Cell Death Dis. 10 (4) (2019) 273.
[51] J. Tommelein, L. Verset, T. Boterberg, P. Demetter, M. Bracke, O. De Wever, Cancer-associated fibroblasts connect metastasis-promoting communication in colorectal cancer, Front Oncol 5 (2015) 63.
[52] H. Cho, Y. Seo, K.M. Loke, S.W. Kim, S.M. Oh, J.H. Kim, et al., Cancer-stimulated CAFs enhance monocyte differentiation and protumoral TAM activation via IL6 and GM-CSF secretion, Clin. Canc. Res. 24 (21) (2018) 5407–5421.
[53] S.P. Rebelo, C. Pinto, T.R. Martins, N. Harrer, M.F. Estrada, P. Loza-Alvarez, et al., 3D-3-culture: a tool to unveil macrophage plasticity in the tumour microenvironment, Biomaterials 163 (2018) 185–197.
[54] T. Yoshimura, E.A. Robinson, S. Tanaka, E. Appella, J. Kuratsu, E.J. Leonard, Purification and amino acid analysis of two human glioma-derived monocyte chemoattractants, J. Exp. Med. 169 (4) (1989) 1449–1459.
[55] G. Comito, E. Giannoni, C.P. Segura, P. Barcellos-de-Souza, M.R. Raspollini, G. Baroni, et al., Cancer-associated fibroblasts and M2-polarized macrophages synergize during prostate carcinoma progression, Oncogene 33 (19) (2014) 2423–2431.
[56] H. Fujimoto, T. Sangai, G. Ishii, A. Ikehara, T. Nagashima, M. Miyazaki, et al., Stromal MCP-1 in mammary tumors induces tumor-associated macrophage infiltration and contributes to tumor progression, Int. J. Canc. 125 (6) (2009) 1276–1284.
[57] A. Tsuyada, A. Chow, J. Wu, G. Somlo, P. Chu, S. Loera, et al., CCL2 mediates cross-talk between cancer cells and stromal fibroblasts that regulates breast cancer stem cells, Canc. Res. 72 (11) (2012) 2768–2779.
[58] T. Yoshimura, E.J. Leonard, Secretion by human fibroblasts of monocyte chemoattractant protein-1, the product of gene JE, J. Immunol. 144 (6) (1990) 2377–2383.
[59] Z.Y. Lin, Y.H. Chuang, W.L. Chuang, Cancer-associated fibroblasts up-regulate CCL2, CCL26, IL6 and LOXL2 genes related to promotion of cancer progression in hepatocellular carcinoma cells, Biomed. Pharmacother. 66 (7) (2012) 525–529.
[60] T. Silzle, M. Kreutz, M.A. Dobler, G. Brockhoff, R. Knuechel, L.A. Kunz-Schughart, Tumor-associated fibroblasts recruit blood monocytes into tumor tissue, Eur. J. Immunol. 33 (5) (2003) 1311–1320.
[61] J. Giri, R. Das, E. Nylen, R. Chinnadurai, J. Galipeau, CCL2 and CXCL12 derived from mesenchymal stromal cells cooperatively polarize IL-10+ tissue macrophages to mitigate gut injury, Cell Rep. 30 (6) (2020) 1923–19234 e4.
[62] S. Torres, R.A. Bartolome, M. Mendes, R. Barderas, M.J. Fernandez-Acenero, A. Pelaez-Garcia, et al., Proteome profiling of cancer-associated fibroblasts identifies novel proinflammatory signatures and prognostic markers for colorectal cancer, Clin. Canc. Res. 19 (21) (2013) 6006–6019.
[63] J. He, Y. Song, G. Li, P. Xiao, Y. Liu, Y. Xue, et al., Fbxw7 increases CCL2/7 in CX3CR1hi macrophages to promote intestinal inflammation, J. Clin. Invest. 129 (9) (2019) 3877–3893.
[64] E. Sierra-Filardi, C. Nieto, A. Dominguez-Soto, R. Barroso, P. Sanchez-Mateos, A. Puig-Kroger, et al., CCL2 shapes macrophage polarization by GM-CSF and M-CSF: identification of CCL2/CCR2-dependent gene expression profile, J. Immunol. 192 (8) (2014) 3858–3867.

[65] M.A. Cannarile, M. Weisser, W. Jacob, A.M. Jegg, C.H. Ries, D. Ruttinger, Colony-stimulating factor 1 receptor (CSF1R) inhibitors in cancer therapy, J Immunother Cancer 5 (1) (2017) 53.
[66] C.A. Gomez-Roca, A. Italiano, C. Le Tourneau, P.A. Cassier, M. Toulmonde, S. P. D'Angelo, et al., Phase I study of emactuzumab single agent or in combination with paclitaxel in patients with advanced/metastatic solid tumors reveals depletion of immunosuppressive M2-like macrophages, Ann. Oncol. 30 (8) (2019) 1381–1392.
[67] B. Ruffell, L.M. Coussens, Macrophages and therapeutic resistance in cancer, Canc. Cell 27 (4) (2015) 462–472.
[68] R. Aguirre-Gamboa, H. Gomez-Rueda, E. Martinez-Ledesma, A. Martinez-Torteya, R. Chacolla-Huaringa, A. Rodriguez-Barrientos, et al., SurvExpress: an online biomarker validation tool and database for cancer gene expression data using survival analysis, PloS One 8 (9) (2013) e74250.